2011

Dissolved organic matter composition and photoreactivity in prairie lakes of the U.S. Great Plains

Christopher L. Osburn
North Carolina State University at Raleigh

Courtney R. Wigdahl
University of Maine - Main

Sherilyn C. Fritz
University of Nebraska-Lincoln, sfritz2@unl.edu

Jasmine E. Saros
University of Maine - Main, jasmine.saros@maine.edu

Limnol. Oceanogr., 56(6), 2011, 2371–2390

doi:10.4319/lo.2011.56.6.2371

Dissolved organic matter composition and photoreactivity in prairie lakes of the U.S. Great Plains

Christopher L. Osburn,[a,*] Courtney R. Wigdahl,[b] Sherilyn C. Fritz,[c] and Jasmine E. Saros[b]

[a] Department of Marine, Earth, and Atmospheric Sciences, North Carolina State University, Raleigh, North Carolina
[b] Climate Change Institute and School of Biology and Ecology, University of Maine, Orono, Maine
[c] Department of Earth and Atmospheric Sciences and School of Biological Sciences, University of Nebraska, Lincoln, Nebraska

Abstract

Dissolved organic matter (DOM) of 27 prairie saline lake ecosystems was investigated in the Northern and Central Great Plains of the United States using absorbance, fluorescence, lignin concentration, and stable C isotope values. The majority of variation in DOM fluorescence among lakes was due to humic (peak C) and microbially formed (peak M) fluorescent components, which appear to be derived from autochthonous primary production. Strong correlations between peak M and nutrients allow us to model total phosphorus (TP) concentration using peak M fluorescence and chromophoric dissolved organic matter (CDOM) absorption. The rate of primary production (PP) was positively correlated with peak M fluorescence and negatively with lignin concentration. Lignin phenol yields in the DOM were generally smaller than those of most freshwater systems. $\delta^{13}C$ values of dissolved organic carbon (DOC) ranged from −25.0‰ to −20.1‰ and were generally enriched relative to typical freshwaters (ca. −27‰). Terrestrial DOM is degraded in prairie lakes, spanning a gradient from mixotrophic to eutrophic, as determined by a color–nutrient model. The photodegradation of autochthonous DOM was significant: CO_2 fluxes from these prairie lakes, modeled from peak M fluorescence, ranged from 5 to 228 mmol C m^{-2} d^{-1} (median, 37 mmol C m^{-2} d^{-1}) and was similar to community respiration estimated from protein fluorescence (median, 50 mmol C m^{-2} d^{-1}). The combined estimates were about 50% of the global mean total C release previously reported for saline lake ecosystems. The implication of these new results is that the global C release from saline lake ecosystems is likely underestimated.

Ranging from ephemeral saline wetlands and playa lakes to deep permanent meromictic lakes, inland saline lakes are diverse and common on most continents in regions of arid climate (Meybeck 1995). The aridity concentrates dissolved solutes (salts, organic compounds, nutrients), and many of these systems are shallow, eutrophic, and receive high amounts of sunlight during summer months. Despite their ubiquity, small lakes and ponds have been ignored in many estimates of global C cycling (Duarte et al. 2008). Saline lakes often have high primary (Salm et al. 2009) and secondary production (Waiser and Robarts 2000, 2004). Organic matter character and cycling in saline lakes remains poorly studied but appears to be strongly influenced by conductivity (salt content; Curtis and Adams 1995) and, at times, dominated by autochthonous dissolved organic matter (DOM) that undergoes substantial microbial transformation (Leenheer et al. 2004), likely in response to nitrogen and phosphorus availability (Ortega-Retuerta et al. 2007). DOM cycling in saline lakes is of interest because saline lakes have the potential to release large amounts of CO_2 to the atmosphere (Duarte et al. 2008; Finlay et al. 2010).

Further, DOM is a critical regulator of lake ecosystem function and originates via allochthonous sources in watersheds or from autochthonous primary production within the system, both sources potentially being modified by bacteria (Findlay and Sinsabaugh 2003). Sunlight can photochemically degrade DOM, potentially increasing its availability to bacteria (e.g., Waiser and Robarts 2004) and/or its mineralization to CO_2 (Osburn and Morris 2003), yet evidence also exits that sunlight can photochemically humify DOM (Kieber et al. 1997; Mayer et al. 2009). In addition to these pelagic processes, labile DOM can be supplied from the littoral zone (Stets and Cotner 2008). Many endorheic lakes fluctuate in salinity, and changes in ionic strength in aquatic ecosystems may alter DOM microbial degradation (Boyd and Osburn 2004) and photochemical reactivity (Osburn and Morris 2003; Osburn et al. 2009). A clearer understanding of how DOM—which forms the basis of the microbial loop in most aquatic ecosystems—responds to evapoconcentration and dilution will provide a context within which to evaluate lake ecosystem function in response to changing and fluctuating climate (e.g., Anderson and Stedmon 2007).

Biogeochemical analyses of DOM in lakes suggests that autochthonous sources are more abundant in carbohydrates and proteins (often measured as total hydrolyzable amino acids) than are allochthonous sources, which are dominated by recalcitrant compounds, such as lignin. Broadly, these DOM sources can be traced using DOM's fluorescence properties (Fellman et al. 2010). The chemical composition of DOM in saline lakes is not well known and may differ from freshwater lakes, in part because of the very different physicochemical environments (e.g., abundance of salts, restricted water input, long hydraulic residence time, and high sunlight exposure), in addition to high primary productivity. Overall, this lack of knowledge on the DOM of saline lakes complicates their characterization within modern lake paradigms of lacustrine structure and function (Williamson et al. 1999).

* Corresponding author: closburn@ncsu.edu

In this paper we characterize DOM in prairie lakes in the U.S. midcontinent along a gradient of conductivity, which we assumed a priori represents the effects of negative hydrologic balance (precipitation minus evaporation). We specifically examined the contribution of autochthonous and allochthonous C sources to DOM in these lakes, to evaluate whether patterns observed in a limited number of saline lakes are widespread. In the Great Salt Lake, for example, DOM was characterized as almost entirely autochthonous, originating from algae and bacteria and having a major fraction composed of oxidized amino sugar derivatives (Leenheer et al. 2004), compounds that can contribute to DOM fluorescence through their microbial and/or photochemical modification (Biers et al. 2007). Additionally, we wanted to define the role of DOM photochemistry in prairie lake carbon cycling. To achieve our objectives, we measured DOM excitation–emission matrix (EEM) fluorescence as a primary means of characterizing DOM (Stedmon et al. 2003; Fellman et al. 2010) and compared these results to DOM chemical properties (carbon stable isotopes and lignin concentrations). We considered the photodegradation of DOM in prairie lakes as a C flux in addition to heterotrophic respiration. This study was part of a larger research project to investigate the effects of DOM on primary production in prairie saline lake ecosystems (Salm et al. 2009) and included ~30 lakes in the Great Plains of the United States, ranging from western Nebraska to eastern North Dakota.

Methods

Study sites—Surface water samples were collected from lakes in the Great Plains in May and August 2004. The limnological characteristics and a summary of optical and chemical properties of DOM for each lake in 2004 are presented in Table 1. (Additional data from June 2001 are included in this study only for Alkali Lake, North Dakota.) Data from a prior study on primary productivity rates and nutrients in these lakes were included with the DOM properties measured in this study (Salm et al. 2009). The central Great Plains (CGP) lakes are located near the Crescent Lake National Wildlife Refuge in southwest Nebraska. The northern Great Plains (NGP) lakes span from North and South Dakota to eastern Montana. Most lakes are sulfate and carbonate dominated (Salm et al. 2009). Apart from the survey of 27 lakes, Alkali Lake, North Dakota (an NGP lake), was sampled in June 2001 and May and August 2004. Water from the 2001 sampling was used in a photobleaching experiment.

Sample handling and measurements—DOM samples were gently filtered through precleaned (18.2 MΩ MilliQ-water rinse) 0.2-μm polyethersulfone membranes (PALL corporation) using a peristaltic pump and precleaned silicone tubing, directly into acid-washed 250-mL polycarbonate bottles and stored in the dark at 4°C. Storage time varied between 2 and 3 weeks, since the sampling period lasted up to 2 weeks. Upon return to the lab, all the samples were measured for chromophoric DOM (CDOM) absorbance using a Shimadzu UV1601 spectrophotometer with MilliQ water as a reference. A 1- or a 5-cm quartz cell was used for all samples, which were corrected for scattering by subtracting the absorbance at 700 nm. The subtracted measured absorbance (A) was converted to Napierian absorption coefficients (a) using Eq. 1.

$$a_{(\lambda)} = 2.303 A_{(\lambda)} / L \quad (1)$$

L was the pathlength of the quartz cell in meters (0.01 or 0.05 m). The spectral slope, S, of the absorption curve over the wavelength range of 300 to 650 nm ($S_{300–650}$) was obtained by fitting Eq. 1 to the measured data using nonlinear regression. The ratio of S calculated from 275 to 295 nm ($S_{275–295}$) to S calculated from 350 to 400 nm, S_R, was also calculated (Helms et al. 2008).

CDOM EEM fluorescence was measured immediately following absorption measurements on a Shimadzu RF5301 spectrofluorometer. Excitation wavelengths ranged from 250 to 450 nm at 5-nm increments, while emission wavelengths were sampled every 1 nm from 300 to 600 nm. EEM fluorescence intensities were corrected for Rayleigh and Raman scattering by Milli-Q water blank-subtraction and for instrument bias prior to correction for any inner-filtering effect (Stedmon and Bro 2008). Finally, each EEM was calibrated to the water Raman signal so that fluorescence is reported in Raman units (nm^{-1}). These corrections were performed using an in-house script written for Matlab. Once processed, EEM files were assembled into a data matrix and modeled by parallel factor analysis (PARAFAC) in Matlab using the DOMFluor toolbox (Stedmon and Bro 2008). PARAFAC uses an alternating least squares process to minimize an error term between measured and modeled EEMs, which are constructed from loadings of three factors corresponding to excitation wavelength, emission wavelength, and fluorescence intensity. No assumptions were made regarding the shape of components decomposed from the data matrix, except for nonnegativity constraints (e.g., negative fluorescence intensity is meaningless in this case). Split-half validation was used to validate the number of components.

Dissolved inorganic carbon (DIC) samples were gently filtered by syringe into 40-mL borosilicate vials to overflowing and then capped tightly with a Teflon-lined septum and stored at 4°C in the dark until shipped back to the laboratory for analysis. Storage time was about 15 d from sampling to analysis. Dissolved organic carbon (DOC) samples were filtered into prcombusted (550°C, 6 h minimum) 40-mL borosilicate vials capped with Teflon-lined septa using the protocol described above and acidified to pH 2–3 with reagent grade H_2SO_4 (Fisher Scientific). These samples were stored at 4°C for ~2–3 weeks prior to analysis after shipment from the field sites.

DIC and DOC concentration and stable isotope values ($\delta^{13}C$) were analyzed separately on a modified analytical system that coupled an OI 1010 total organic carbon wet chemical oxidation (WCO) carbon analyzer to a Thermo Delta PlusXP isotope ratio mass spectrometer (WCO-IRMS; Osburn and St-Jean 2007). DIC measurements were conducted on 0.1–2-mL aliquots in which 5% H_3PO_4 was added to the sample in the reaction chamber of the TOC

Table 1. Location and limnological data for the lakes in this study. Sp. Cond. = specific conductance.

Lake	State	Latitude (°N)	Longitude (°W)	Area (km^2)	Sp. Cond. ($mS\ cm^{-1}$)	DIC ($mg\ L^{-1}$)	DOC ($mg\ L^{-1}$)	Chl *a* ($\mu g\ L^{-1}$)	TP ($\mu g\ L^{-1}$)	TN ($\mu g\ L^{-1}$)
Northern Great Plains										
East Stump	North Dakota	47.868	98.353	21.53	9.67	83.0	28.2	14.0	173	2798
East Devils	North Dakota	47.960	98.612	23.55	5.56	102.0	28.5	6.6	273	2145
Horseshoe	North Dakota	47.836	98.790	3.95	4.77	173.3	28.2	5.8	108	2499
Free People	North Dakota	47.911	98.719	2.18	6.93	211.0	32.4	13.2	71	2705
Stink	North Dakota	48.265	99.224	2.23	7.62	88.7	28.7	2.0	228	2583
Alkali	North Dakota	48.581	103.586	1.85	11.50	374.2	47.7	22.0	251	4379
Kettle	North Dakota	48.608	103.624	0.03	1.75	116.6	13.4	14.4	30	694
Isabel	North Dakota	46.820	99.752	4.54	1.39	110.2	21.5	18.0	51	969
George	North Dakota	46.738	99.495	5.78	16.20	257.8	32.6	14.6	70	1621
Alkaline	North Dakota	46.668	99.567	28.03	3.90	143.2	23.7	5.8	58	1379
Coldwater	North Dakota	46.011	99.068	2.37	1.99	68.6	18.4	13.2	42	1063
Brush	Montana	48.600	104.111	1.07	5.83	258.4	22.2	1.1	19	587
Clear	Montana	48.651	104.143	1.13	7.20	315.1	56.6	7.3	46	1908
Goose	Montana	48.834	104.060	0.82	53.50	809.1	319.6	550.0	1710	16,645
Hazelden	South Dakota	45.515	97.433	3.59	4.40	71.8	27.6	1.6	134	2374
Waubay	South Dakota	45.446	97.382	46.94	2.20	86.3	14.2	18.2	71	1180
Bitter	South Dakota	45.267	97.268	55.85	3.06	87.0	25.6	5.8	149	1596
Medicine	South Dakota	44.978	97.358	1.07	14.50	83.3	24.4	4.8	206	1875
Albert	South Dakota	44.531	97.136	14.97	1.85	38.0	25.5	4.5	104	2378
Central Great Plains										
Alkali	Nebraska	41.819	102.598	0.56	1.66	274.1	112	3.0	243	997
Island	Nebraska	41.735	102.398	2.07	0.58	59.7	34.4	35.6	711	4009
Joe	Nebraska	42.210	102.606	0.61	4.98	326.8	80.2	3.7	400	4487
Border	Nebraska	41.794	102.536	0.11	72.81	12,605.0	*	23.4	15,860	23,297
Goose	Nebraska	41.778	102.445	0.80	9.62	870.3	328.6	36.2	3567	20,514
Jim	Nebraska	42.204	101.901	0.36	1.58	156.9	110.6	2.6	501	3804
Patterson	Nebraska	42.003	102.382	0.50	39.05	3405.0	*	16.5	5382	21,259
Wickson	Nebraska	42.160	102.589	0.24	15.67	1683.3	*	21.0	4238	20,671
Mean				840	11.47	846.6	61.9	32.0	1285	5571
Minimum				3	0.58	38.0	13.4	1.1	19	587
Maximum				5585	72.81	12,605.0	328.6	550.0	15,860	23,297
Median				208	5.56	156.9	28.4	13.2	173	2378

* Values not reported because of probable contamination with DIC.

analyzer and heated to 80°C for 2 min. The CO_2 formed was then sparged from solution past a nondispersive infrared (NDIR) detector to quantify DIC concentration (in mg C L^{-1}), and then swept in a stream of ultrahigh-purity (UHP) He to the IRMS for $\delta^{13}C$ measurement. DOC measurements were made on 0.3- to 1-mL samples (depending on DOC concentration) after presparging with UHP He for 10 min to remove inorganic C prior to analysis. On some samples containing large amounts of DIC (up to 1200 mg L^{-1}), the sparging time was extended up to 8 h. The CO_2 evolved after heated persulfate oxidation was measured with a protocol similar to that for DIC. Calibration of carbon concentrations was achieved with the response of potassium hydrogen phthalate solutions of known concentration (1 to 100 mg L^{-1}); relative standard deviations were <3% over this range of DOC concentrations. The smaller sample volumes described above were used to place the response of high DOC samples within this calibration curve range for the NDIR detector, and appropriate adjustments for sample size were made to get the actual concentrations. Carbon stable isotope values of DIC and DOC are reported as $\delta^{13}C$ in per mil units (‰):

$$\delta^{13}C = \left(R_{samp} - R_{ref}/R_{ref}\right) \times 1000 \quad (2)$$

where R_{samp} is the ratio of $^{13}C:^{12}C$ for the sample and R_{ref} is the ratio of $^{13}C:^{12}C$ of CO_2 reference gas. Carbon isotope values were normalized to the Vienna Pee Dee Belemnite international scale using solutions of oxalic acid (−18.3‰) and L-glutamic acid (−26.2‰), and reproducibility of $\delta^{13}C$ measurements was ±0.4‰.

Lignin phenols were used as biomarkers for vascular plant contribution (terrestrial organic matter) to DOM on 23 lakes in May 2004. Roughly 500 mL of 0.2-μm filtrates was acidified and extracted onto C_{18} resin in the field following Louchouarn et al. (2000). The extracts were eluted from the columns in the laboratory using high-purity methanol and evaporated to dryness in 150-mL Teflon reaction vessels then hydrolyzed in 2 mol L^{-1} NaOH via microwave-assisted CuO oxidation in an inert atmosphere of N_2 (Goni and Montgomery 2000). Trans-cinnamic acid was added as a recovery standard, and lignin oxidation products were quantified on a five-point calibration of eight individual phenol standards. Separation of lignin phenols was performed on an Agilent G1530A 6890 series gas chromatograph (GC) fitted with a RTX-5MS capillary column (30 m, 0.25-mm inner diameter; Restek), and detection was performed using an Agilent 5973 mass selective detector. Lignin was quantified as the sum of eight vanillyl, syringyl, and cinnamyl phenols (Σ_8) and normalized to DOC concentration (Λ_8). The ratios of syringyl to vanillyl phenols (S:V) and cinnamyl to vanillyl phenols (C:V) were used to indicate vascular plant tissue type. The ratio of acid to aldehyde phenols in the vanillyl group $(Ad:Al)_v$ was used to indicate oxidative degradation.

Photobleaching experiment—Water from Alkali Lake, North Dakota, was used in photobleaching experiments to determine changes to DOM caused by natural sunlight exposure, following methods in Osburn et al. (2009). Filtered water samples were placed into baked (550°C, 5 h) quartz bottles closed with ground glass stoppers and sealed on the outside with parafilm. The bottles were submerged in a flowing water bath at a depth of 3 cm and exposed to natural sunlight for 2 d. Bottles wrapped in foil also were exposed to natural sunlight as dark controls. After the exposure period, DOC concentration, DOM absorption, and EEM fluorescence were measured.

Results

General lake characteristics—DOM optical and chemical characteristics varied widely among the lakes surveyed; several lakes had very large DOC and CDOM concentrations, in addition to high conductivity. The limnological characteristics of the lakes are presented in Table 1, and specific optical and chemical properties are presented in Table 2. Median values are reported in both tables to show the influence of high conductivity lakes on the mean values of the properties studied. Both the lowest conductivity (0.6 mS cm^{-1}) and the highest conductivity (72.8 mS cm^{-1}) were measured for the CGP lakes (Island Lake and Border Lake, Nebraska, respectively). In general the CGP lakes were shallow (<2 m), while the NGP lakes ranged in depths from 1 to 13 m (Salm et al. 2009). The CGP lakes were also smaller in size, most <1 km^2, while the NGP lakes often exceeded 1 km^2. Bitter Lake, South Dakota, was the largest lake sampled (55.8 km^2). Goose Lake, Montana, had the highest conductivity of the NGP data set and was similar in many respects to the CGP lakes. The attenuation coefficient for photosynthetically active radiation (PAR), $K_{d\mathrm{PAR}}$, averaged 1.99 m^{-1}, and the median value was 1.69 m^{-1}, values similar to Canadian prairie lakes (Arts et al. 2000).

DOC concentrations—DOC concentrations ranged from 13.40 mg L^{-1} (Kettle Lake, North Dakota) to 328.6 mg L^{-1} (Goose Lake, Nebraska; Table 1). These values are toward the upper end of DOC concentrations across most lake ecosystems (Sobek et al. 2007), but they are consistent with saline lakes and wetlands (Arts et al. 2000; Mariot et al. 2007). Three lakes had extremely high DOC concentrations, >500 mg L^{-1} (Border Lake, Wickson Lake, and Patterson Lake, all in Nebraska), which may have indicated contamination from DIC, and were removed from further analysis involving DOC-related results. Lakes less than 1.00 km^2 had DOC concentrations ranging from 20 to 328.6 mg L^{-1}, except for Kettle Lake, North Dakota. The median DOC concentration was 28.4 mg L^{-1}, lower than the mean DOC concentration of 61.9 mg L^{-1}; the latter value is skewed by the high DOC concentrations in Goose Lake, Montana, and Goose Lake, Nebraska. A log–log regression of DOC concentration on lake area was not significant.

CDOM absorption and fluorescence—CDOM absorption at 350 nm (a_{350}) was lowest (1.7 m^{-1}) for Brush Lake, Montana, and highest (123.98 m^{-1}) for Patterson Lake, Nebraska (Table 2). Similar to DOC concentration, the

Table 2. Chemical and optical data for the lakes in this study. Σ_8 = sum of eight lignin phenols; Λ_8 = sum of lignin phenols normalized to 100 mg organic C; $K_{d\mathrm{PAR}}$ = light attenuation coefficient for photosynthetically active radiation (PAR), integrated from 400–700 nm; $F_{\max}$ = maximum fluorescence intensity (Raman units). nd = not determined.

Lake	Σ_8 (μg L^{-1})	Λ_8 mg (100 mg C)$^{-1}$	δ^{13}C-DIC (‰)	δ^{13}C-DOM (‰)	$K_{d\mathrm{PAR}}$ (m^{-1})	a_{350} (m^{-1})	$S_{300-650}$ (μm^{-1})	$S_{275-295}$ (μm^{-1})	$S_{350-450}$ (μm^{-1})	S_R	$F_{\max}$ (nm^{-1})	HIX	BIX
Northern Great Plains													
East Stump	83.80	0.97	−4.2	−22.9	1.25	10.56	25.71	22.18	21.40	1.04	2.44	4.51	0.81
East Devils	56.70	0.199	−3.6	−23.7	1.82	7.48	25.71	28.69	22.27	1.29	2.77	3.69	0.85
Horseshoe	88.10	0.312	−2.5	−24.4	1.53	13.06	23.48	25.36	19.95	1.27	2.74	4.26	0.72
Free People	96.06	0.296	−1.3	−23.7	1.41	10.84	21.78	25.15	18.92	1.33	2.25	2.71	0.78
Stink	96.00	0.334	−3.7	−22.8	2.28	9.93	24.78	26.17	21.64	1.21	3.29	3.67	0.80
Alkali, North Dakota	72.20	0.151	−3.5	−23.1	4.05	12.43	28.19	30.46	22.80	1.34	3.58	3.05	0.84
Kettle	52.50	0.392	0.0	−24.5	1.78	4.14	26.03	29.24	22.05	1.33	1.20	2.24	0.84
Isabel	42.70	0.199	0.1	−24.2	nd	3.76	29.14	33.31	23.60	1.41	1.12	2.10	0.85
George	46.94	0.144	−1.1	−22.4	nd	5.53	27.49	32.70	22.81	1.43	1.68	2.73	0.91
Alkaline	51.83	0.219	−1.8	−24.0	nd	12.43	28.19	33.03	22.41	1.47	1.35	2.43	0.84
Coldwater	30.28	0.165	−2.5	−24.6	1.69	4.94	27.16	31.97	22.51	1.42	1.42	2.56	0.83
Brush	32.00	0.144	−2.1	−23.6	0.48	1.81	34.84	34.80	24.28	1.43	0.43	1.88	0.92
Clear	37.10	0.066	−0.7	−25.0	1.30	2.52	35.29	40.76	22.28	1.83	0.76	1.39	0.91
Goose	30.90	0.010	1.6	−22.3	nd	15.06	41.23	40.82	24.50	1.67	10.08	1.47	1.02
Hazelden	nd	nd	−4.6	−23.4	0.95	8.85	26.67	28.26	23.46	1.20	3.11	4.34	0.81
Waubay	38.00	0.268	−3.3	−24.0	2.47	5.08	25.7	29.33	22.55	1.30	2.00	2.37	0.83
Bitter	64.26	0.251	−2.6	−23.3	1.73	8.25	26.24	28.41	22.51	1.26	2.50	3.53	0.86
Medicine	66.54	0.273	−1.7	−20.5	0.90	8.00	24.6	27.16	21.78	1.25	2.49	3.23	0.89
Albert	36.06	0.141	−4.6	−24.1	nd	6.30	26.48	28.01	22.46	1.25	1.68	3.67	0.82
Central Great Plains													
Alkali, Nebraska	27.00	0.024	1.7	−22.3	nd	24.99	25.93	25.32	19.95	1.27	5.41	5.98	0.73
Island	nd	nd	6.3	−20.1	6.23	38.08	23.67	31.65	19.09	1.66	1.80	6.08	0.69
Joe	29.30	0.037	−2.2	−22.5	nd	79.30	28.45	26.88	20.46	1.31	6.61	4.44	0.74
Goose	60.60	0.018	1.6	−22.5	nd	74.63	29.66	31.96	23.265	1.37	8.33	2.56	0.94
Jim	nd	nd	nd	−21.5	nd	80.96	26.25	29.08	21.89	1.33	8.65	6.44	0.72
Patterson	nd	nd	0.1	nd	nd	123.98	39.04	29.93	22.270	1.34	14.02	3.32	0.84
Wickson	49.90	nd	−2.0	nd	nd	68.66	31.23	36.06	25.874	1.39	6.73	5.05	0.73
Mean	55.09	0.172	−1.4	−22.8	1.99	26.49	28.61	30.28	22.27	1.36	3.79	3.45	0.83
Minimum	27.00	0.003	−4.6	−25.0	0.48	1.81	21.78	22.18	18.92	1.04	0.43	1.39	0.69
Maximum	96.06	0.392	6.3	−19.5	6.23	123.98	41.23	40.82	25.87	1.83	14.02	6.44	1.02
Median	51.83	0.165	−1.92	−23.1	1.69	10.6	26.7	29.33	22.41	1.33	2.49	3.27	0.84

average a_{350} (26.49 m^{-1}) was much larger than the median a_{350} (10.6 m^{-1}). However, the spectral slope (S) values, which are a qualitative indicator of the rate at which CDOM absorption declines with increasing wavelength over various wavelength ranges, were distributed over a narrower range. The minimum $S_{300–650}$ value was 21.35 ± 0.02 μm^{-1} (Free Peoples Lake, North Dakota), while the maximum $S_{300–650}$ value was 42.1 ± 1.2 μm^{-1} (Goose Lake, Montana). Further, unlike DOC concentration or a_{350}, the mean $S_{300–650}$ value (28.61 μm^{-1}) was much closer to the median $S_{300–650}$ value (26.70 μm^{-1}). The distribution of values for $S_{275–295}$ and $S_{350–400}$ was very similar to that for $S_{300–650}$ (Table 2). The average S_R value was 1.36, very similar to the median value of 1.33. East Stump Lake had the minimum S_R value (1.04), while Clear Lake had the maximum S_R value (1.83).

Like S values, maximum fluorescence (F_{max}) values were also distributed over a narrow range. The median F_{max} was 2.49 nm^{-1}, while the mean F_{max} was 3.79 nm^{-1}. However, Brush Lake, Montana, had the lowest F_{max} (0.43 nm^{-1}), whereas Patterson Lake, Nebraska, had the highest F_{max} (14.02 nm^{-1}). Thus, the most absorptive and fluorescent material was found in Patterson Lake, Nebraska, and the least absorptive and fluorescent material was found in Brush Lake, Montana. These lakes were different from Border Lake, Nebraska, which had the highest DOC concentration, and Kettle Lake, North Dakota, which had the lowest DOC concentration.

EEM fluorescence variation among lakes—Five representative EEMs from the lakes are shown as contour plots in Fig. 1, both for May 2004 and August 2004 samplings. The dominant peak in each lake occurred at an excitation nm : emission nm ratio (Ex : Em) of Ex 250 : Em 380–460, which corresponds to the ultraviolet (UV) humic-like peak A (Table 3; Fellman et al. 2010), but which also has been observed in microbial and photochemical modification of amino sugars (Biers et al. 2007) and in marine phytoplankton cultures (Romera-Castillo et al. 2010). Secondary peaks were observed at Ex 275 : Em 340 (peak T) in Brush Lake and Clear Lake. Lake George is representative of most lakes surveyed and has a pattern consistent with typical freshwater DOM fluorescence. Peak A dominates, but a strong secondary signal at Ex 320–360 : Em 420–460 (peak C) also is observed, most often as a plateau, as is a shoulder into peak T. Goose Lake, Montana, DOM exhibits a different pattern in the dominant fluorescent regions of its EEM. While peak A is prevalent and dominant in May 2004, this lake showed the development of a longer wavelength peak in August centered on Ex 300 : Em 400 nm. This peak corresponds to peak M in Table 3 and was the dominant peak in several lakes from the CGP. Peak M was the strongest signal in DOM fluorescence in high conductivity lakes and had a strong relationship to nutrients and DOC over a wide geographical and limnological distribution of lakes from near freshwater (e.g., Kettle Lake, Montana) to hypersaline (Border Lake, Nebraska). Another prominent feature of the Goose Lake EEM fluorescence in August 2004 was the shoulder extending out to soil fulvic-like fluorescence at Ex 390 : Em 509 (peak D) and a nearly discrete peak at Ex 435 : Em 535. The latter feature is likely a component of humic acid-like fluorescence (Fellman et al. 2010).

Some overlap between terrestrial and autochthonous DOM fluorescence peak assignments occurs. Several marine phytoplankton groups grown in axenic cultures produced strong peak T and peak M fluorescence (Romera-Castillo et al. 2010). Microbial and photochemical modification of autochthonous DOM also appears to generate fluorescence that overlaps with terrestrial sources. Sunlight photohumification of labile substrates produced fluorescence similar to peak C (Kieber et al. 1997), whereas microbial and photochemical processing of amino sugars in seawater produced peak A, peak C, and peak M fluorescence (Biers et al. 2007). However, in the latter study, these features were transient and quickly disappeared upon further sunlight exposure. In coastal upwelling systems, strong peak M and peak T fluorescence attributed to microbial processes has been observed (Nieto-Cid et al. 2006; Milbrandt et al. 2010).

Fluorescence-derived indices—Ratios of fluorescence intensity over specific regions have been used to provide a snapshot of DOM source and reactivity. The humification index (HIX) describes DOM's age and recalcitrance, while the biological index (BIX) describes a contribution of autochthonous DOM to natural waters (Birdwell and Engel 2010). HIX showed a wider degree of variation (1.39 to 6.44) for the study lakes than did BIX (0.69–1.02), but lakes having high HIX values had correspondingly low BIX values. For example, Goose Lake, Nebraska, had the highest HIX value (6.44), but one of the lowest BIX values (0.72), while Goose Lake, Montana, had one of the lowest HIX values (1.47) and the highest BIX value (1.02). The range of HIX and BIX values are bracketed between fulvic acids from algal-dominated Pony Lake, Antarctica (18 and 1.5, respectively; Birdwell and Engel 2010) and a chlorophyte-dominated algae culture (0.22 and 2.09, respectively, C. Osburn unpubl. data).

PARAFAC model results—Using PARAFAC, a five-component model was split-half validated for the NGP and CGP lakes. In order to achieve the validation, several lakes (Goose Lake, Montana; Border Lake, Nebraska; Goose Lake, Nebraska; Jim Lake, Nebraska; Patterson Lake, Nebraska; and Wickson Lake, Nebraska) had to be removed from the data set because their calculated leverages (a computation relating any individual sample to the average of the data set) were close to one, indicating their uniqueness from the rest of the data set (Stedmon and Bro 2008). The results of the split-half validation are shown as the loadings for each component in the two halves randomly selected from the total data set (Fig. 2). Each half of the data was modeled separately for five components; each component is ranked one to five in terms of the amount of variance that component explained for the overall model. For each component, both halves are nearly identical, indicating a valid choice of the number of components derived by the PARAFAC model. Component 4 had the weakest match between halves for the excitation loading.

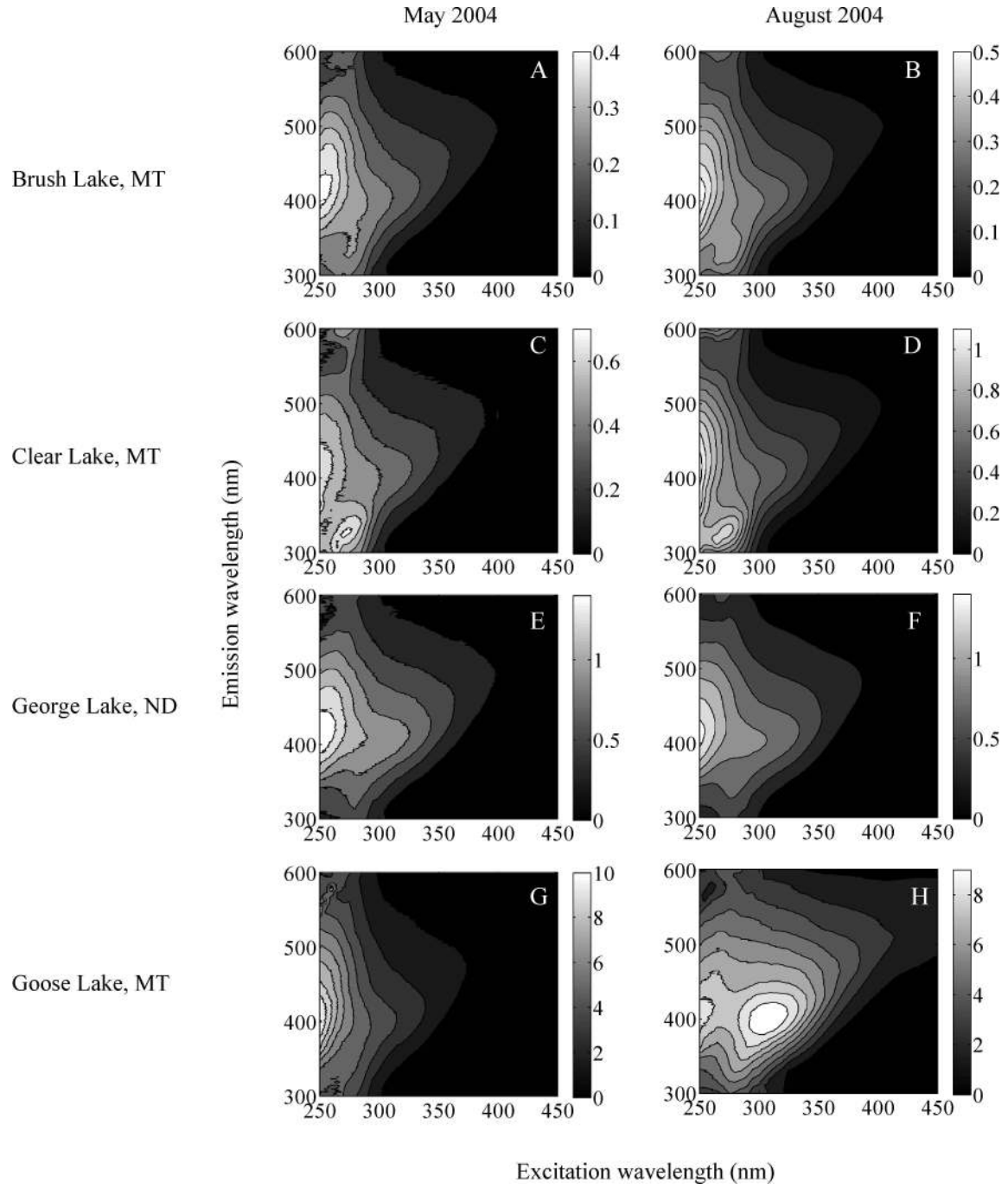

Fig. 1. EEM contour plots for select lakes from the NGP, showing the contrast in EEM fluorescence between May and August in 2004. Color bar is fluorescence intensity in Raman units (R.U.).

Table 3. Excitation and emission fluorescence maxima of the five components identified by the PARAFAC model and compared with previously identified fluorescent regions. Wavelengths in parentheses are secondary maxima. Closest analogues are the fluorescent peaks identified in earlier works and summarized in table 1 of Stedmon et al. (2003).

Component number	Excitation max (nm)	Emission max (nm)	Closest analogue	Correlation coefficient (r)	Probable source and/or reactivity in this study
1	270 (340)	450	peak C	0.992	terrestrial humic-like; photolabile
2	305 (<250)	400	peak M	0.985	microbial humic-like
3	<250	432	peak A	0.985	terrestrial humic-like; refractory
4	280 (390)	510	peak D	0.941	ubiquitous soil fulvic-like
5	280	324	peaks B or T	0.947	autochthonous protein-like

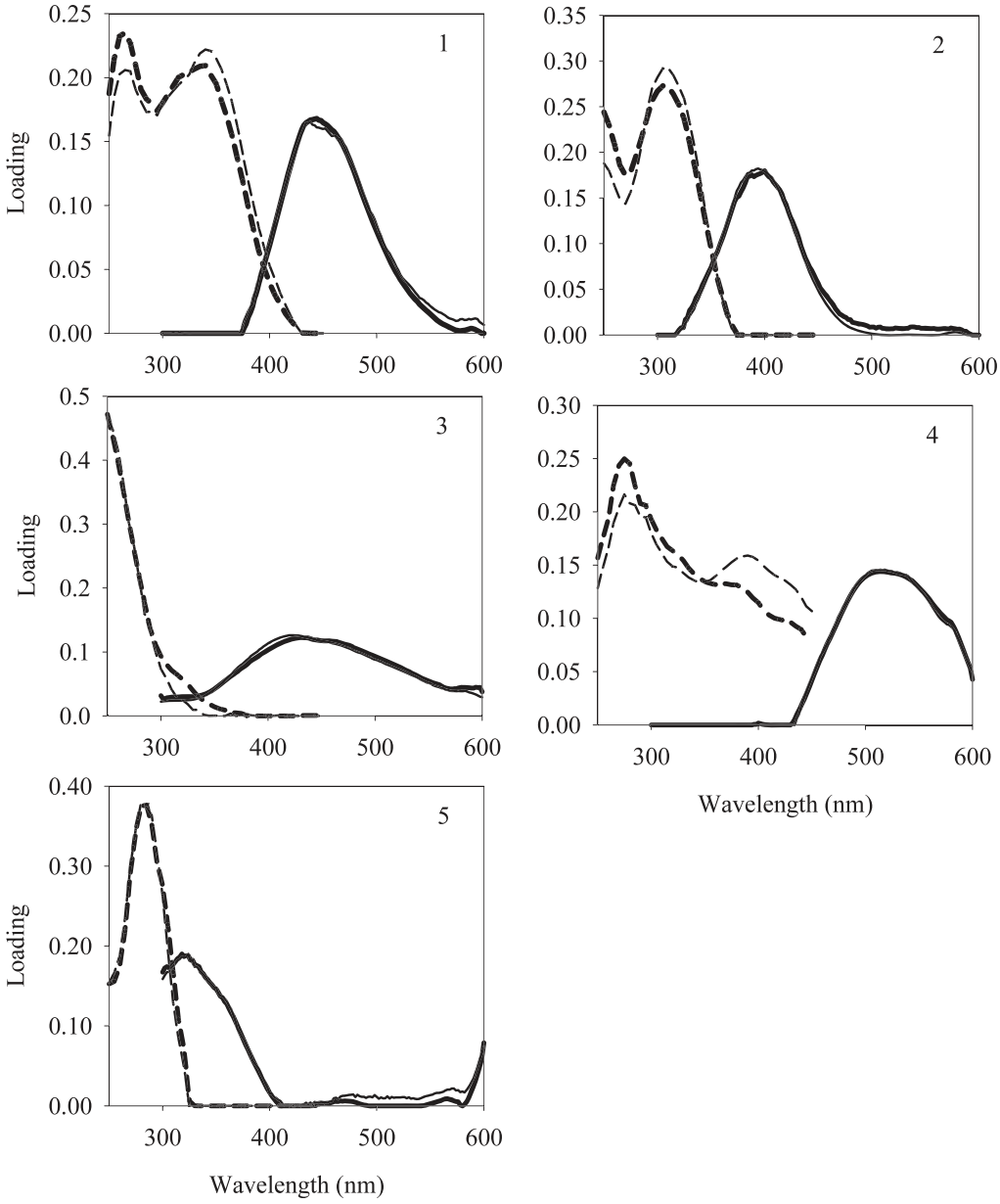

Fig. 2. PARAFAC model output of five components identified in the NGP and CGP data set. Components 1–5 are in order of decreasing amount of variance explained by the model (1 = highest; 5 = lowest). Excitation (dashed lines) and emission (solid lines) spectra are shown, as are the results from the split-half validation (thin and thick lines, respectively).

The validated model components correspond to previously identified EEM fluorescence regions (Table 3). Three of five components identified by PARAFAC were mainly of terrestrial origin (C1, C3, and C4) and corresponded to the peaks C, A, and D, respectively. C2 resembles peak M, identified as microbially transformed autochthonous DOM (Fellman et al. 2010). Finally, C5 corresponds to protein-like fluorescence, but the emission maximum at 324 nm was not resolved into either tryptophan fluorescence (emission at 340 nm) or tyrosine fluorescence (emission maximum at 304 nm).

Visual inspection of the distribution of F_{max} values for each component of the PARAFAC model revealed several trends (Fig. 3). First, despite the variability explained, the F_{max} values are mostly ranked C3 > C2 > C1 > C5 > C4, or, in terms of peak assignments, A > M > C > T > D. This pattern generally held for 17 of the 21 lakes in the model, though in one case (Horseshoe Lake, North Dakota), the F_{max} values for C1 and C2 (peak C peak M) were equal. Notable exceptions to this trend were observed for two lakes from NGP and two lakes from CGP. For Brush Lake, Montana, the C5 (peak T) was second in terms of F_{max}, while for Clear Lake, Montana, this component had the highest F_{max} value. In both of these lakes, C1 (peak C) was only greater in fluorescence than C4 (peak D). In the CGP lakes, Alkali Lake, Nebraska, had a higher C4 (peak D) F_{max} value than C5, while Island Lake, Nebraska, had C3 > C1 > C2 > C4 = C5. That is, the F_{max} value of

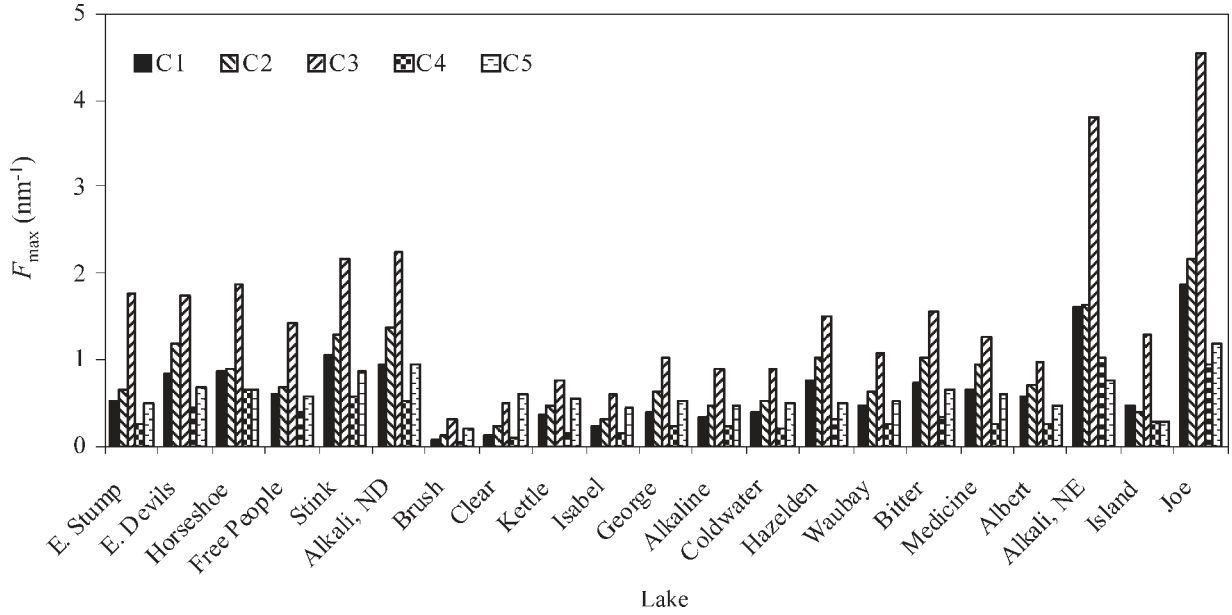

Fig. 3. Variation in maximum fluorescence for C1–C5 for each lake in the data set.

soil fulvic-like fluorescence was equal to the F_{max} of protein fluorescence.

Because several lakes had to be removed from the PARAFAC model, the Pearson's correlation coefficient was calculated between each component of the PARAFAC model and the corresponding EEM peak (i.e., closest analogue). The components were highly correlated to the regions of DOM EEM fluorescence previously identified, so further analysis of EEM fluorescence data will focus on these analogues.

Carbon stable isotopes—Dissolved carbon pool stable isotope values showed a strong influence of ^{13}C-enrichment in the DIC and DOC of the CGP lakes relative to the NGP lakes (Table 2). Carbon stable isotope values of DIC ranged from −4.6 to +6.3‰ with a median δ^{13}C–DIC value of −1.9‰. There was no significant relationship with DIC concentration, which ranged from 38 mg L^{-1} (Lake Albert, South Dakota) to 12,605 mg L^{-1} (Border Lake, Nebraska; Table 1). DOC stable isotopes (mean = −23.1‰, Table 2) were enriched relative to typical temperate freshwater lake DOC values (−26‰ ± 1.5‰, Osburn et al. 2001). The most depleted δ^{13}C–DOC value was −25.0‰ (Clear Lake, Montana), and the most enriched δ^{13}C–DOC value was −20.1‰ (Island Lake, Nebraska). The variation in δ^{13}C–DOC values could not be explained by increasing DOC concentrations (r^2 = 0.11, p = 0.050, df = 22). However, the NGP lakes showed a significant enrichment of δ^{13}C–DOC value with conductivity (r^2 = 0.44, p = 0.0013, df = 17). By contrast, the CGP lakes showed no significant trend in δ^{13}C–DOC value with conductivity.

Nutrients and chlorophyll—Total nitrogen (TN), total phosphorus (TP), and chlorophyll *a* (Chl *a*) concentration data from Salm et al. (2009) were included as an estimate of nutrient loads to each lake. Both TN and TP concentrations were greatest in Border Lake, Nebraska, and lowest in Brush Lake, Montana (Table 1). Chl *a* values ranged from 1.1 μg L^{-1} (Brush Lake, Montana) to 550.0 μg L^{-1} (Goose Lake, Montana). The mean Chl *a* concentration was 32.0 μg L^{-1}, while the median value was 13.2 μg L^{-1}. Goose Lake, Montana, was a clear outlier in terms of algal biomass. This lake was bright green in color and heavily dominated by the chlorophyte *Dunaliella* sp. (Salm et al. 2009).

Dissolved lignin—Absolute concentrations of the eight lignin phenols (Σ_8: vanillyl + syringyl + cinnamyl phenols) were lowest in Alkaline Lake, Nebraska (27 μg L^{-1}), and highest in Free Peoples Lake, North Dakota (96.1 μg L^{-1}) (Table 2). Yields of dissolved lignin (Λ_8: mg lignin per 100 mg OC) provide an indication of the fraction of DOC that is terrestrial and ranged from 0.010 for Goose Lake, Montana, to 0.392 for Kettle Lake, North Dakota. Dissolved lignin S : V vs. C : V ratios suggested a mixture of vascular plant tissue types lacking in gymnosperm nonwoody tissue (Fig. 4A). The dissolved lignin from both NGP and CGP lakes was somewhat depleted in angiosperm woody tissue and angiosperm nonwoody tissue (leaves and grasses) sources. This effect appears stronger in the CGP lakes. Grasses are rich in cinnamyl phenols and typically plot in the "a" region of Fig. 4A. The highest C : V ratio (0.13) was found for lignin in Alkali Lake, North Dakota, while the lowest C : V ratio (0.00) was found for Clear Lake, Montana. This indicated that Clear Lake was notably lacking in cinnamyl phenols, which is surprising given the dominance of grasslands in the Great Plains. The oxidative state of dissolved lignin indicated by $(Ad : Al)_v$ ratios was lowest (0.56) for East Stump and Kettle Lakes (both in North Dakota), while the highest ratio (1.16) was found for Medicine Lake, Nebraska. This ratio was positively correlated to conductivity (r^2 = 0.20, p = 0.019; n = 23), but the trend was strongly driven by data from only two lakes (Fig. 4B).

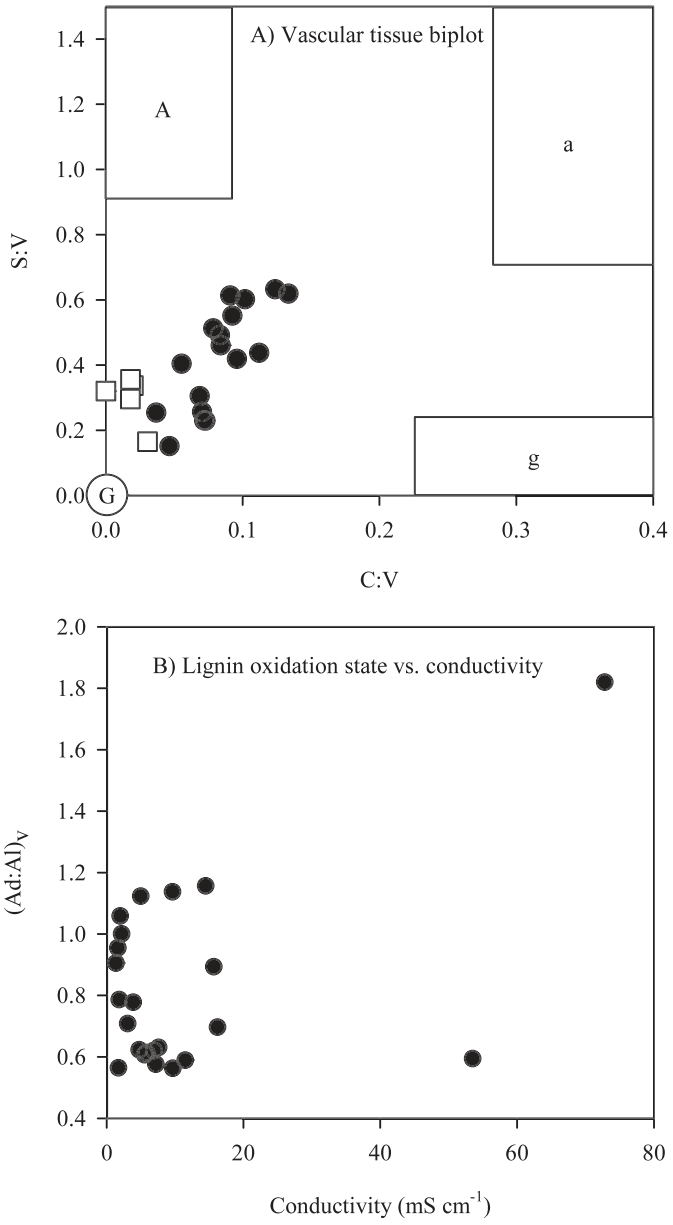

Fig. 4. (A) Plot of syringyl : vanillyl (S : V) vs. cinnamyl : vanillyl (C : V) phenol ratios for DOM in surface waters of lakes from the NGP and CGP. Shaded boxes are the compositional ranges for major plant tissues (Hedges and Mann 1979). G = gymnosperm woody tissue; g = gymnosperm nonwoody tissue (needles); A = angiosperm woody tissue; a = angiosperm leaves and grasses. (B) Plot of vanillic acid to vanillin (aldehyde) ratios against conductivity for DOM from the NGP and CGP lakes.

Trends with conductivity—At most, conductivity explained just over 20% of the variation in any of the optical or chemical properties reported when all lakes were pooled together (data not shown). Most notably, DOC-specific absorption at 350 nm, a^*_{350}, decreased with conductivity ($\log a^*_{350} = -0.313 + 0.402 \times \log$ conductivity; $r^2 = 0.26$; $p = 0.006$; $n = 24$). However, separating the NGP from the CGP lakes revealed similar trends and significant models among many variables (Table 4). Except for S_R, HIX, and BIX, each variable was log transformed prior to regression calculations. DOC increased in both lake groups, although the trend was only significant for the NGP lakes. For both NGP and CGP lakes, F_{max} increased significantly with conductivity but a_{350} did not. The qualitative indicators for CDOM absorption, S_R and a^*_{350}, also did not show a trend when the lakes were separated into groups. HIX showed a significant decrease with conductivity in the CGP lakes, but no significant trend in the NGP lakes was found. By contrast, BIX increased significantly with conductivity in both lake groups, although the degree of variance explained was greater in the CGP lakes (60%) than in the NGP lakes (24%). Conductivity explained 50% and 60% of the variation in TN for NGP and CGP lake groups, respectively. Much greater variation in TP was explained by conductivity (72%) in the CGP lakes than in the NGP lakes (40%). Conductivity was not a significant predictor of Chl *a* concentration in either lake group. The concentration of lignin phenols, Σ_8, was not significantly related to conductivity for the NGP lakes, although it was for the CGP lakes, where conductivity explained about 80% of the increase in Σ_8. The opposite trend was found for Λ_8, in which the CGP lakes showed no significant relationship

Table 4. Linear regression statistics for the explanation of DOM and nutrient properties by conductivity. All values were log transformed, except for variables marked with †, so the general form of the regression equations is log (Y) = m × log (C) + b, where Y = DOM or nutrient property, C = conductivity, m = slope coefficient, and b = intercept. Significance level was 95%; slope coefficients and intercept values are not shown for *p* greater than 0.05.

Y	Adjusted r^2	*p*	*n*	m	b
NGP lakes					
DOC	0.59	<0.001	19	0.572	1.055
a_{350}	0.17	0.082	19	—	—
a^*_{350}	0.12	0.081	19	—	—
†S_R	0.00	0.327	19	—	—
F_{max}	0.24	0.019	19	0.387	0.0143
†HIX	−0.05	0.752	19	—	—
†BIX	0.24	0.019	19	0.084	0.787
TN	0.50	<0.001	19	0.921	2.664
TP	0.40	0.002	19	0.725	1.489
Chl *a*	0.11	0.089	19	—	—
Σ_8	−0.03	0.542	18	—	—
Λ_8	0.28	0.014	18	−0.508	−0.380
CGP lakes					
DOC	0.58	0.085	5	—	—
a_{350}	0.28	0.101	8	—	—
a^*_{350}	0.40	0.150	5	—	—
†S_R	−0.06	0.466	8	—	—
F_{max}	0.66	0.016	7	0.314	0.523
†HIX	0.54	0.037	7	−1.566	6.251
†BIX	0.60	0.025	7	0.097	0.682
TN	0.61	0.013	8	0.570	3.430
TP	0.72	0.005	8	0.782	2.570
Chl *a*	−0.01	0.372	8	—	—
Σ_8	0.77	0.032	5	0.299	1.358
Λ_8	−0.08	0.837	3	—	—

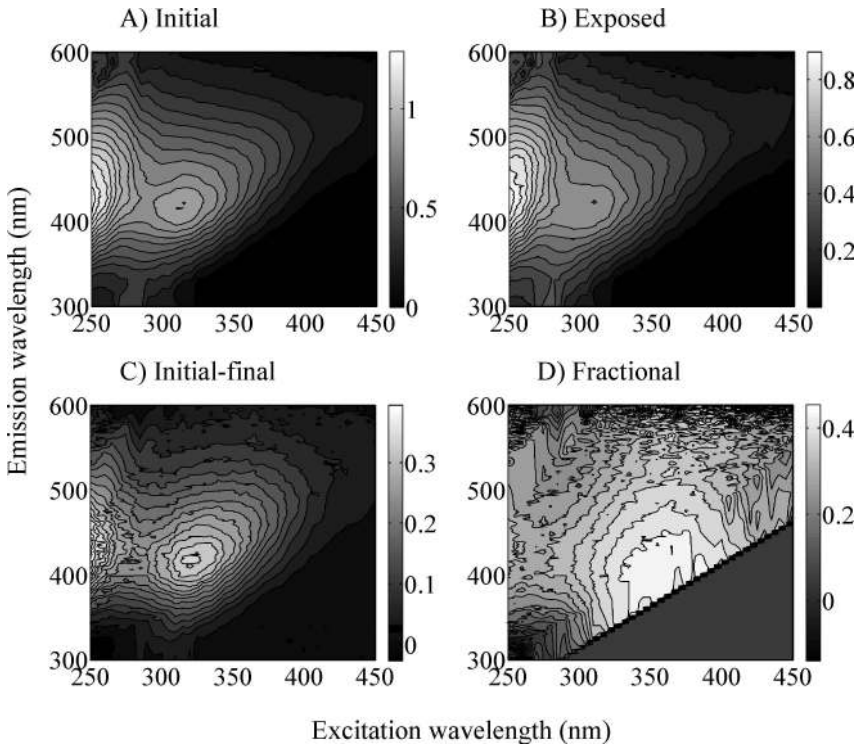

Fig. 5. Comparison of EEM contour plots of Alkali Lake, North Dakota, showing the spectral effects of photodegradation on DOM fluorescence. In all plots, the color bar indicates intensity of fluorescence. (A) Initial sample prior to exposure; (B) after 2 d sunlight exposure; (C) a subtracted contour plot showing the main photobleaching at the peak A and peak C regions; (D) a plot showing the fractional photobleaching, with higher values indicating relatively more photobleaching (despite absolute fluorescence lost, as shown in C).

with conductivity, yet a weak ($r^2 = 0.28$) negative trend was found for the NGP lakes. However, the NGP lake trend was caused primarily by Goose Lake, Montana, and once this lake was removed, the regression was not significant.

DOM photodegradation—Sunlight exposure of filtered water from Alkali Lake, North Dakota (collected in June 2001), for 2 d caused distinct changes to its DOM (Fig. 5A–5D). DOC concentration decreased by 14% (43.6 to 36.8 mg C L^{-1}), while a_{350} decreased by 36%. The rate coefficient for photooxidation of DOC to DIC was 2.49 mg C L^{-1} d^{-1}. Both peak C and peak A were most photolabile, since F_{max} at each peak decreased by approximately 0.3 nm^{-1} (Fig. 5C). However, the relative photobleaching of these peaks was not equivalent. Peaks C and M, which lost 41% and 36% of initial fluorescence, respectively, experienced a relatively greater amount of photobleaching than did peak A, which decreased by 29%. The protein peaks exhibited the least amount of photobleaching: peak T decreased by 9% and peak B by 2%. In Fig. 5D, the most fractional photobleaching of DOM fluorescence (>40%) occurred in the region of peak C, overlapping peaks M and N.

Photodegradation also changed the quality of DOM from Alkali Lake, North Dakota. After 2 d of sunlight exposure a^*_{350} decreased by 26% and $S_{300–650}$ values increased by 20%. Most of this change in spectral slope occurred in the low ultraviolet wavelengths as $S_{275–295}$ increased by 17%, while $S_{350–400}$ increased by 4%. The slope ratio (S_R) increased from 1.24 to 1.41, consistent with CDOM photobleaching (Helms et al. 2008). The HIX ratio decreased by 5%, while the BIX ratio decreased by 2%.

Discussion

An important finding from this study is that autochthonous DOM, as indicated by fluorescence, accumulates in a broad geographic range of prairie lakes having widely different chemical properties. The EEMs and PARAFAC-derived components from our Great Plains data set generally resemble EEMs and PARAFAC components published elsewhere for freshwater lakes, streams, wetlands (*see* review by Fellman et al. 2010), and saline ponds in the Brazilian Patanal wetland (Mariot et al. 2007). Also, F_{max} values from the PARAFAC model showed that, while peak C and peak M (C1 and C2, respectively) captured most variation across lakes, peak A (C3) was generally the most fluorescent (Fig. 3). A surprising result was the relatively high photolability of peaks C and M, which were highly correlated to nutrients and appear to be autochthonously derived (Table 5), relative to the terrestrial humic peak A (Fig. 5). Despite this finding, it is clear that Great Plains prairie lakes contain large amounts of terrestrial organic matter, relative to DOC, as shown by our lignin results.

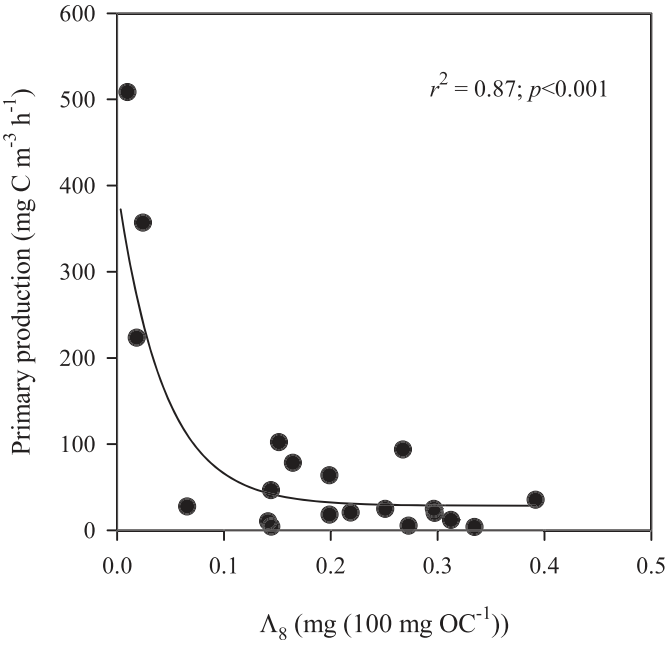

Fig. 6. The rate of primary production (PP) decreased with increasing fraction of the DOC as lignin. PP data were obtained from Salm et al. (2009).

Effect of conductivity on DOM in prairie lakes—Conductivity clearly indicated the evapoconcentration of DOM and nutrients in both the NGP and CGP lake groups (Table 4). While CDOM absorption at 350 nm did not increase significantly with conductivity, F_{max} and DOC did in both the NGP and CGP lake groups. This implies that evapoconcentration does have some effect on the quantity of DOM in lakes with high conductivity, as noted for prairie lakes in Alberta, Canada (Curtis and Adams 1995; Arts et al. 2000). The slopes of the log DOC–log conductivity regressions for our lake groups (NGP and CGP) were compared with regressions we calculated from prior work on saline lake DOM (Table 6). Across a range of saline lakes, the slope of the log–log regression is surprising similar, 0.534 ± 0.127, and conductivity explained 56–77% of the variability in DOC concentration. This consistency of the slope values among these regressions demonstrates the importance of evapoconcentration for shaping the amount of DOM found in saline lakes globally.

The quality of DOM also changes with evapoconcentration, although the effect was seen more strongly for the CGP lakes than the NGP lakes. Across the Great Plains lakes, DOM became more autochthonous in nature with increasing conductivity, yet the concentration mechanism also appeared to increase terrestrial DOM in the Sand Hills lakes of Nebraska. This assertion is supported by the increase in BIX ratios with conductivity observed for both lake groups and a decrease in the HIX ratio with conductivity only for the CGP lakes. However, lignin also increased in the CGP lakes with conductivity but not as a fraction of DOC concentration. Both N and P are also concentrating in these lakes, possibly because of differences in land use, which would supply ample nutrients to sustain both phytoplankton and bacterial production (Salm et al. 2009). These results suggest two possibilities: that terrestrial DOM was diluted by autochthonous production, or that terrestrial DOM was heavily degraded as conductivity increases in these lakes. We discuss each possibility in turn.

Autochthonous DOM in prairie lakes—Rates of primary production (PP) in the lakes were significantly lower when lignin comprised a larger fraction of the DOM (Fig. 6) but not when CDOM absorption comprised a larger fraction of DOC, i.e., a^*_{350} (data not shown). This result is somewhat surprising, and using a multiple linear regression test, we found that PP was best modeled with peak M, which had a positive influence on PP, and lignin concentration, which had a negative effect on PP ($\log PP = 5.105 + 1.169 \times \log M + 2.151 \times \log \Sigma_8$; $r^2 = 0.57$; $p < 0.001$; RMSE = 0.3955; $n = 21$). The significant terms were determined by forward stepwise regression with no model terms, adding in the most statistically significant term (the one with the lowest p) until the root mean squared error (RMSE) of the model was reached. A second stepwise regression of DOC on fluorescence resulted in peak T and peak M being the best predictors of DOC concentration ($\log DOC = 1.126 + 0.237 \times F_{max,T} + 0.109 \times F_{max,M}$; $r^2 = 0.76$; $p < 0.001$; RMSE = 0.2979; $n = 21$). This analysis explains the overall increase in BIX with conductivity seen in these lakes (Table 4).

The preceding argument is supported by DOM fluorescence–nutrient relationships. Higher primary production and more nitrate were found in the CGP lakes compared with the NGP lakes (Salm et al. 2009). Both TP and TN, as well as conductivity, had higher correlation coefficients to peaks C, M, and N than to either the protein peaks B or T, or the terrestrial humic peak A (Table 5). Further, peak M was strongly related to CDOM absorption ($M = 0.675 + 0.068a_{350}$; $r^2 = 0.78$, $p < 0.001$; $n = 26$), and, using both, we

Table 5. Matrix of Pearson correlation coefficients for nutrients and conductivity with DOM EEM fluorescence peaks. All values indicate a significant correlation ($p < 0.05$); ns = not significant. Peak assignments are the same as Table 2.

	EEM fluorescence peak labels						
Parameter	B	T	A	C	M	N	D
TN	0.81	0.78	0.80	0.86	0.87	0.85	0.50
TP	0.52	0.53	0.45	0.78	0.76	0.60	0.50
Conductivity	0.72	0.76	0.54	0.63	0.65	0.69	ns

created a bio-optical model of TP concentration for the lakes in our data set:

$$\log \mathrm{TP} = 1.3563 + 0.867 \times \log \mathrm{M} + 0.7706 \times \log a_{350}$$
$$\left(r^2 = 0.80; \mathrm{RMSE} = 0.3335; n = 26\right) \quad (3)$$

This model shows the importance of peak M as a qualitative indicator of autochthonous DOM in relation to nutrient and DOM concentrations in lakes. Peak M was a prominent feature of microbial fulvic acids from Antarctic lakes lacking terrestrial DOM inputs (McKnight et al. 2001) and is a ubiquitous microbial DOM signal related to primary production and found in many marine, coastal, and inland environments (Stedmon et al. 2003). Similar microbially derived fulvic acids identified in the Great Salt Lake fit a model best described as oxidized amino sugar acids (Leenheer et al. 2004), which is very compelling when compared with the dominance of peak M in microbially and photochemically modified amino sugars (Biers et al. 2007). Peak M also has also been shown to develop in actively growing and axenic phytoplankton cultures (Romera-Castillo et al. 2010). In light of these reports, the fluorescence results we have shown suggest a changing prominence of autochthonous DOM across the Great Plains prairie lakes, despite the more intense fluorescence from the ubiquitous C3 (terrestrial humic peak A) seen in Fig. 3. The substantial amount of Chl *a* in many of these lakes also supports our assertion that autochthonous DOM was created as a result of bacterial processing of primary production in these lakes.

Carbon isotopes in prairie lake DOM—Carbon stable isotope evidence suggested a mixture of primary production and C3 and C4 land plants as sources to the prairie lakes. For example, Goose Lake, Montana, had a δ^{13}C-DIC value of +1.5‰, and the C3 chlorophyte (*Dunaliella* sp.) that dominates this lake would likely exert a 20‰ fractionation factor on DIC fixed into its biomass. This would produce a phytoplankton δ^{13}C–DOC of −18.5‰.; the δ^{13}C–DOC value of Goose Lake, Montana, was −22.6‰. Thus, a simple mixing model would require that Goose Lake, Montana, DOM be 57% terrestrial and 43% autochthonous based on a terrestrial end-member (C3 land plant) with a δ^{13}C–DOC of −27‰. However, δ^{13}C-POC values of −19.5‰ to −23.6‰ for rivers in the central United States indicate a dominance of C4 grasslands (Onstad et al. 2000). Therefore, mixtures of both C3 and C4 vegetation, thus a mixture of grassland vegetation, deciduous forest vegetation, and phytoplankton, could produce the δ^{13}C–DOC values we measured in many of the Great Plains lakes (Table 2).

However, no relationship was found between δ^{13}C–DOC and Λ_8 that would indicate DOM stable isotope values are depleted when lignin increased as a fraction of DOC. Thus, a trend unrelated to adding terrestrial C must be driving the change in δ^{13}C–DOC values. The δ^{13}C–DIC values showed a clear positive trend with δ^{13}C–DOC (Fig. 7A). Simultaneously, δ^{13}C–DIC values increased with the rate of primary production (Fig. 7B). These results mean that

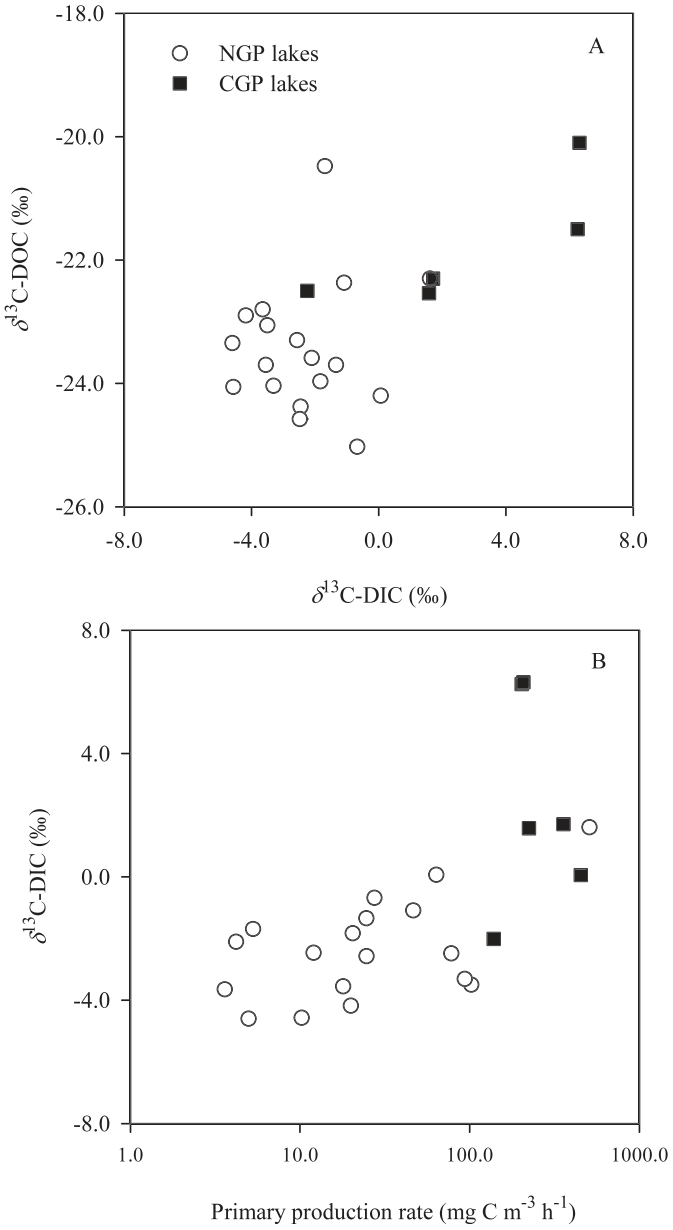

Fig. 7. (A) The relationship between stable carbon isotope composition of DOM and DIC. (B) The δ^{13}C–DIC increased with rate of primary production (values from Salm et al. 2009).

high amounts of primary production in the lakes we studied, formed from isotopically enriched DIC, accumulate in the DOM pool. This is not surprising when examining Goose Lake, Montana, which had nearly 200 times more Chl *a* than lignin, low HIX and high BIX values, and very high concentrations of nutrients (Tables 1 and 2).

Moreover, combining CDOM absorption and stable isotope results suggested that, as CDOM increased relative to DOC, its source was autochthonous production (Fig. 8A,B). Our analysis is based on the work of Blair et al. (2003), who used δ^{13}C values and organic carbon : surface area ratios to express the mass balance of organic

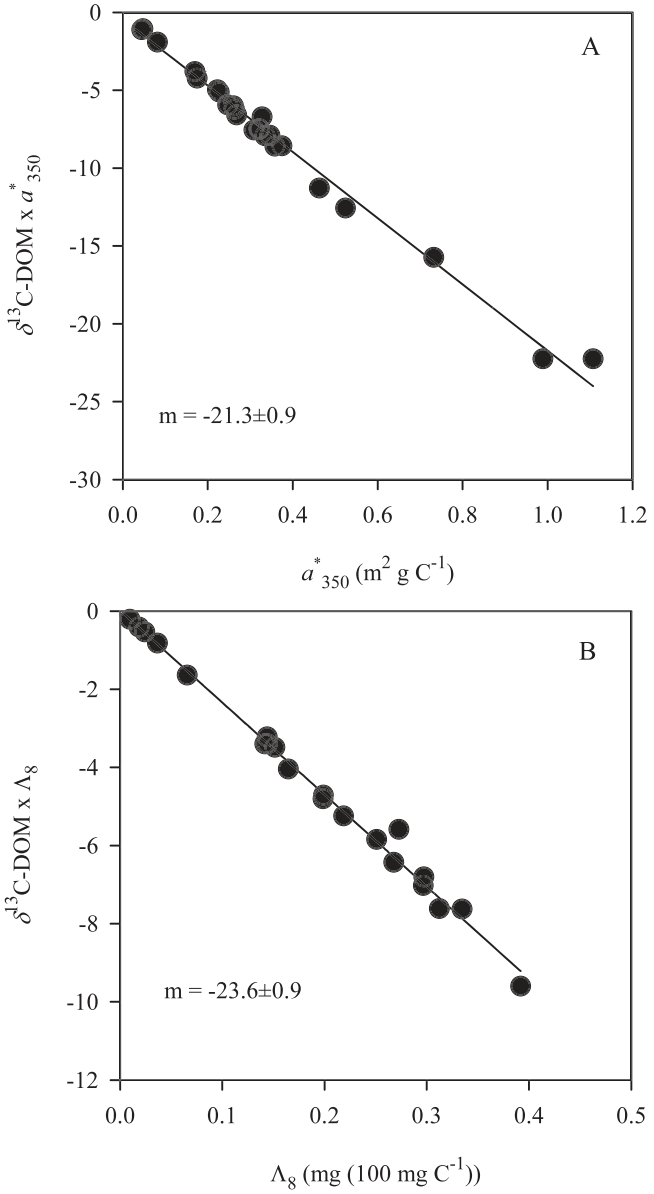

Fig. 8. Carbon stable isotopic signatures for DOM sources in prairie lakes of the U.S. Great Plains. The slope (m) of best-fit lines represents the average (± 1 σ) δ^{13}C values for the DOM responsible for (A) the increase in CDOM absorption as a fraction of DOC concentration, and (B) the increase in lignin as a fraction of DOC concentration.

carbon mixing on a continental shelf (*see* their equations 1–3). Here, we consider the following mass balance equations

$$\delta_l c_l = \delta_t c_t + \delta_a c_a \quad (4)$$

$$c_l = c_t + c_a \quad (5)$$

where δ_l is the δ^{13}C value of lake DOM, and δ_a and δ_t are the δ^{13}C values of the autochthonous and terrestrial carbon inputs. The total increase in CDOM as a fraction of DOC, a^*_{350}, in the lakes as originating from terrestrial and autochthonous sources, is given as c_l, c_a, and c_t, respectively. Equations 4 and 5 are combined and rearranged to produce the mass balance:

$$\delta_l c_l = \delta_a c_l + c_t(\delta_t - \delta_a). \quad (6)$$

The slope of this equation, δ_a, is determined from a plot of $\delta_l c_l$ vs. c_l (Fig. 8A) and was determined to be $-21.3‰ \pm 0.9‰$. This represents the isotopic signature of the carbon responsible for the increase in a^*_{350}, and the value is consistent with the enriched δ^{13}C–DOC values that reflected high rates of primary production in the lakes of the Great Plains.

A similar mass balance was calculated using Λ_8 values in place of a^*_{350} values to determine the average δ^{13}C–DOC value responsible for the added lignin as a fraction of DOC (Fig. 8B). The δ_a in this case was $-23.6‰ \pm 0.9‰$, which was significantly depleted compared with the a^*_{350} -based value. While both estimates of δ^{13}C–DOC values fall within the ranges of terrestrial organic matter expected for the U.S. Great Plains (Onstad et al. 2000) and autochthonous organic matter, they were significantly different. While evapoconcentration has apparently concentrated terrestrial DOM in the CGP lakes, terrestrial DOM has also decreased as a fraction of DOC concentration. Thus, we suggest that the increase in CDOM as a function of DOC in these lakes is due to autochthonous processes.

Trophic status and prairie lake DOM—The nutrient–color paradigm used to describe freshwater lake DOM by Williamson et al. (1999) provides a framework for evaluating prairie lake DOM in the context of trophic status and mixing of autochthonous and terrestrial DOM sources. "Four corners" of a CDOM–nutrient matrix were defined using a_{320} and TP concentrations to maintain consistency with the Williamson et al. matrix (Fig. 9A,B). The dystrophic region of high CDOM and low TP represents very humic "brown" freshwater lakes dominated by terrestrial inputs, whereas purely autochthonous "green" lakes have low CDOM and high TP. In this matrix, Brush Lake, Montana, was included as an example of a eutrophic (high TP, low CDOM) system, but compared with other prairie lakes in our data set, Brush Lake had the lowest Chl *a*, TP, and TN concentrations. Brush Lake's TP and Chl *a* values are low in a broader sense among lakes in general, plotting at the lower end of the classic Chl *a* vs. TP trend (Dillon and Rigler 1974). Moreover, the 1% PAR light depth for Brush Lake was 9.59 m. Brush Lake does not meet criteria for a eutrophic system in chlorophyll–TP space, but this lake and the majority of the lakes studied here fall between states of eutrophy and mixotrophy (high nutrients, high CDOM) in CDOM–TP space. The majority of prairie lakes plotted in the latter region (Fig. 9A). Replacing a_{320} with peak M fluorescence produced a very similar trend with TP concentrations (Fig. 9B). This means that the prairie lakes do not fit well into the Williamson nutrient–color paradigm. Rather, the integration of DOC into trophic evaluations for the prairie lakes strongly suggests the DOC is autochthonous in nature.

That most of the lakes in our dataset were mixotrophic explains the surprising positive correlation between DOM

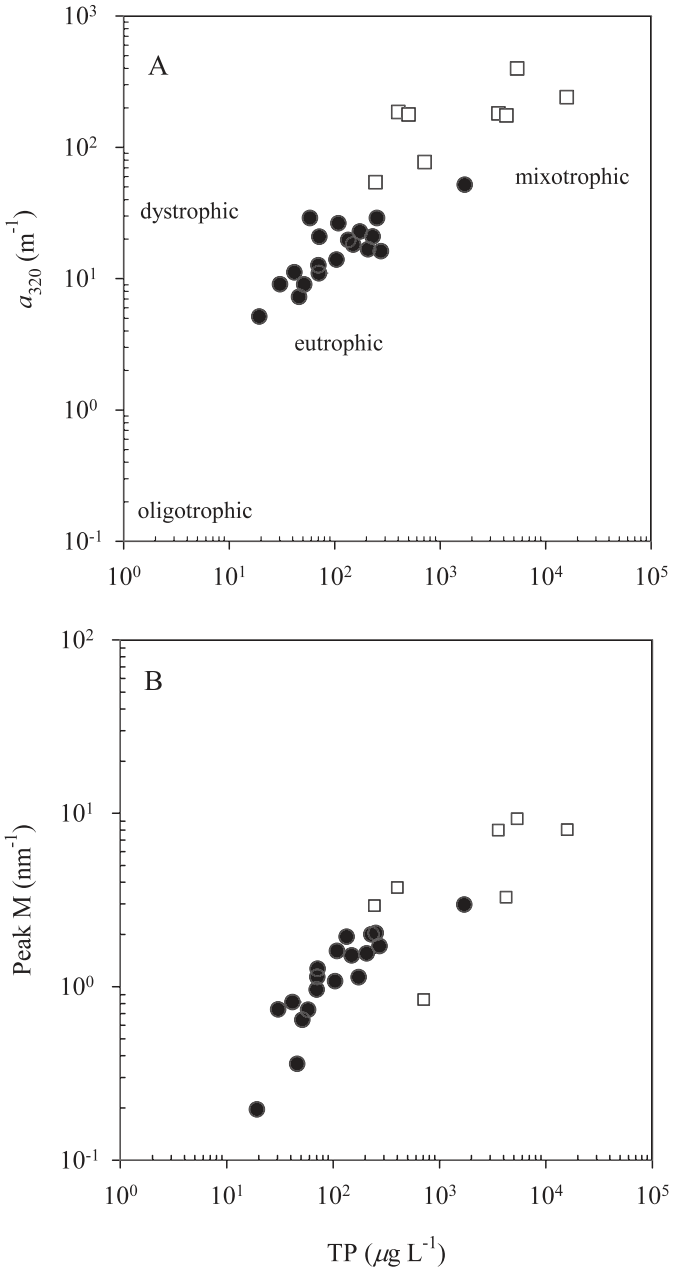

Fig. 9. (A) The nutrient–color paradigm model from Williamson et al. (1999) modified for the higher CDOM and TP values in the majority of the lakes in this study. Most lakes ranged between eutrophic and mixotrophic designations. (B) The increase in log peak M fluorescence, indicating microbially produced autochthonous DOM, plotted as a function of log TP concentration. In both figures, black circles are the NGP lakes and open squares are the CGP lakes.

optical properties (absorbance, fluorescence) and PP and supports the lignin and stable isotope analyses previously discussed. The fluorescence characteristics of C1 and C2 from the PARAFAC model very closely resemble microbial fulvic acids identified for autochthonous-dominated Antarctic lakes (McKnight et al. 2001), and the fluorescence of pore water DOM centered near Ex 360, Em 450 from a eutrophic lake dominated by diatom production (Heinsalu et al. 2007). We did not measure pore waters in the NGP or CGP lakes, but the most productive lakes in our data set were shallow eutrophic systems that may have DOM influenced by pore water release of autochthonous, microbially transformed material.

Photochemical reaction mechanisms in prairie lake DOM—A second important finding from our research was the high amount of photoreactivity attributable to a microbially transformed, autochthonous DOM source in Alkali Lake, North Dakota. The decrease in a^*_{350} and HIX along with increases in spectral slope and S_R values after sunlight exposure was consistent with photodegradation of humic DOM (Helms et al. 2008). A plot of a^*_{350} vs. $S_{300–650}$ values for the prairie lake DOM we studied showed a pattern that was very similar to that found for Greenland saline lakes (Anderson and Stedmon 2007) (Fig. 10A). These authors distinguished the effect of photobleaching on the Greenland lakes as having relatively low DOC-specific absorption and relatively high $S_{300–650}$ values. Waiser and Robarts (2004), who first documented the ability of photodegradation to affect strongly the DOM cycle in saline ponds, also found that $S_{290–420}$ increased while a^*_{350} decreased after sunlight exposure. However, neither S_R nor its component slope coefficients showed a trend with a^*_{350} that would indicate photobleaching in the same manner as did $S_{300–650}$ (Fig. 10B–D).

The losses in DOM fluorescence after Alkali Lake water was exposed to natural sunlight were similar to those reported for photobleaching experiments on whole and fulvic acid–fractionated lake water in the Arctic (Cory et al. 2007) and a variety of freshwater lakes and marshes, in addition to a commercially available humic acid (Winter et al. 2007). In these studies, the majority of fluorescence photobleaching occurred in the peak C and peak A regions, which explains the decrease in the HIX ratio we observed. The rate constant for DOC photooxidation in Alkali Lake was ca. 2.5 mg C L^{-1} d^{-1}, which was much greater than the rate found for a saline wetland in Canada (Waiser and Robarts 2004). Regardless, both studies show the highly photolabile DOM in prairie lake ecosystems. What is notable about our findings for Alkali Lake was that peaks C and M both responded with similar degrees of photobleaching and greater than terrestrial humic DOM (peak A). During senescence of macroalgae, fluorescence signals develop at peaks M and N and then decrease, shifting to peak C (Parlanti et al. 2000). In light of development of peak C in Goose Lake, Montana, and the similar photoreactivity of peak C and M in Alkali Lake, this argues strongly for peak C having autochthonous origins. These results demonstrate that the formation of autochthonous CDOM in prairie lakes can be readily degraded after exposure to sunlight, and our rates indicate this organic C eventually can be oxidized to CO_2.

Curtis and Adams (1995) argued that selective removal of certain DOM pools could occur in lakes situated in semiarid regions and that removal and addition mechanisms are not mutually exclusive. This would appear to be the case in the Great Plains prairie lakes as a result of photochemical degradation and formation of fluorescent

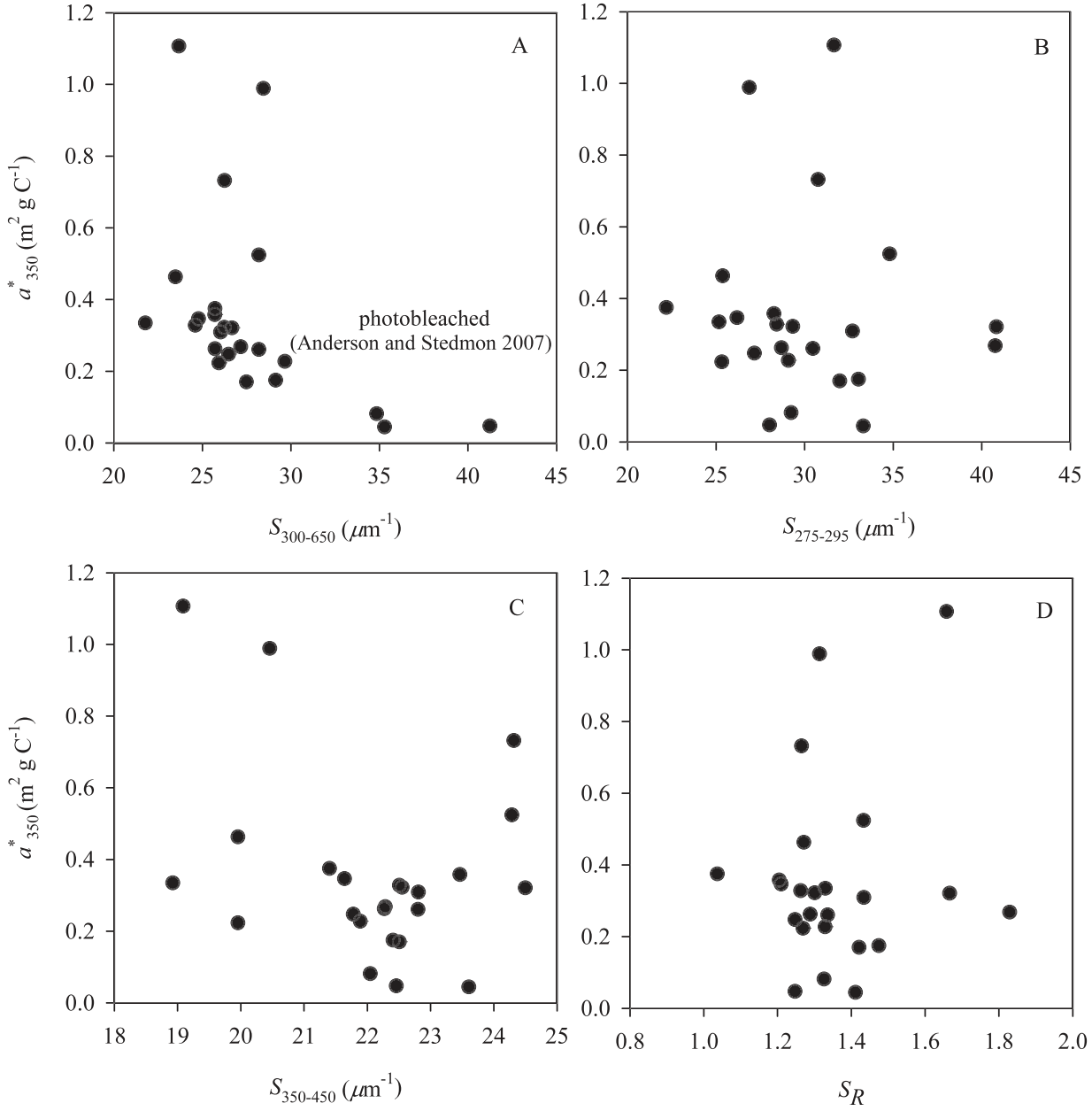

Fig. 10. (A–C) The change in a^*_{350} plotted against the change in S values calculated over various wavelength ranges and (D) against S_R. Lower a^*_{350} values and larger S values indicate photobleached material (Anderson and Stedmon 2007).

humic substances. Σ_8 increased significantly with conductivity only for the CGP lakes, implying that these lakes concentrate terrestrial DOM more than do the NGP lakes, in which Σ_8 did not vary significantly with conductivity (Table 4). The terrestrial fraction of DOM in the high conductivity prairie lakes from our study appears to be quite low, despite the similarity of the median Σ_8 concentration (51.8 μg L^{-1}) to that of rivers (e.g., Congo River, 76.5 μg L^{-1}; Spencer et al. 2009) or any concentrating effect seen with conductivity. Lignin phenol yields per milligram of DOC (Λ_8) were at most 0.392 mg (100 mg OC^{-1}) (Kettle Lake, North Dakota) and as low as 0.010 mg (100 mg OC^{-1}) (Goose Lake, Montana; Table 1). The higher end of these values is similar to late summer Λ_8 values reported for a series of boreal lakes (Ouellet et al. 2009), while the lower end of the lignin phenol yields (<0.1 mg (100 mg OC)$^{-1}$) approach those found in river DOM subjected to substantial photodegradation (0.03 mg (100 mg OC^{-1}); Spencer et al. 2009).

An increase in a^*_{350} with Λ_8 ($r = 0.59$, $p = 0.005$, $n = 21$) suggests that relatively CDOM-poor lakes had relatively less lignin, an effect attributable to photodegradation of terrestrial DOM compounds such as lignin (Spencer et al. 2009). The lignin biomarkers studied from these lakes also indicated effects from photodegradation. First, Λ_8 decreased as a function of conductivity, meaning that less terrestrial, lignin-rich DOM was present in the higher conductivity lakes. Second, the S : V ratio was positively

Table 6. Comparison of DOC–conductivity relationships among saline lakes globally. Regressions from regions other than this study were calculated on data presented in the referenced study (data were estimated averages from Mariot et al. 2007). ns = not significant.

Geographical location	Equation	r^2	P	n	Source
Canadian prairie	log DOC=1.384+0.322×log conductivity	0.56	<0.001	44	Arts et al. (2000)
Southeastern Spain	log DOC=0.809+0.519×log conductivity	0.77	0.009	7	Ortega-Retuerta et al. (2007)
Greenland	log DOC=1.69+0.643×log conductivity	0.61	<0.001	54	Anderson and Stedmon (2007)
Brazilian Pantanal	log DOC=0.364+0.796×log conductivity	0.92	0.001	6	Mariot et al. (2007)
Northern Great Plains	log DOC=1.055+0.572×log conductivity	0.59	<0.001	19	this study
Central Great Plains	log DOC=1.782+0.612×log conductivity	0.58	ns	5	this study

correlated to Λ_8 (Pearson's $r = 0.57$, $p = 0.007$, $n = 21$), as was C : V ratio ($r = 0.64$; $p = 0.002$; $n = 21$), indicating that both syringyl and cinnamyl phenols were relatively lower in DOM for which lignin was a small fraction (Joe Lake, Nebraska, was removed as a statistical outlier). A simple dilution of lignin concentration would not change S : V or C : V ratios; the selective removal of vanillyl, syringyl, or cinnamyl phenols would change these ratios. The cinnamyl phenols are probably removed as terrestrial DOM is transported through soils (Ouellet et al. 2009). Photochemistry likely does not remove cinnamyl phenols at rates sufficient to influence C : V ratios, and the removal of syringyl phenols during DOM photodegradation tends to be size dependent (Hernes et al. 2007). This variability with DOM size probably explains a weak correlation we found between S : V and a^*_{350} ($r = 0.42$; $p = 0.05$, $n = 21$). However, the $(Ad : Al)_v$ values of lignin from the Great Plains lakes were relatively constant and did not suggest that highly oxidized lignin occurred in these lakes, a result also found in boreal lakes (Ouellet et al. 2009). A variety of fractionation processes between phase transfers of organic matter (leaching and sorption) likely restricts the utility of $(Ad : Al)_v$ ratios to compare oxidative states of lignin among our study lakes (Hernes et al. 2007). Rather, $(Ad : Al)_v$ measured seasonally within each lake might better indicate changes to lignin due to photodegradation.

In addition to photodegradation, photohumification may be occurring in the nutrient-rich and highly productive prairie lakes, especially as a result of the presence of N. Photochemistry has also been shown to oxidatively cross-link lipid precursors, creating a peak C fluorescence signal and incorporating N into the newly formed marine humic substances (Kieber et al. 1997). Peak M tends to emerge after the photodegradation of algal detritus, which also was linked to N incorporation of amines and free ammonia (Mayer et al. 2009), the latter probably significant at the pH of these lakes (Table 1). Further, Mayer et al. (2009) argued that tryptophan (peak T) photoproducts are photolabile. This supports a highly photolabile peak M observed during amino sugar microbial and photochemical processing (Biers et al. 2007). It is thus probable that photochemistry is both forming and degrading CDOM in saline lakes, which would explain the change in EEMs from Goose Lake, Montana, between May and August 2004, which exhibited a shift from peak A toward the regions of peaks M and C (Fig. 1G,F). The large concentrations of TN in the NGP and CGP lakes mean that photohumification certainly is possible.

In general, our observational data suggest active biogeochemical cycles of autochthonous and allochthonous DOM in saline lakes. As conductivity increases, so does DOC, but our evidence suggests most of this DOC enrichment is due to autochthonous production in these eutrophic and mixotrophic lakes and that activity also produces fluorescent material, as suggested by a color–nutrient model (Fig. 9A,B) and as reported in the literature (Nieto-Cid et al. 2006; Biers et al. 2007; Romera-Castillo et al. 2010). Both microbial and photochemical processes likely cause the increase in peak M fluorescence, which itself is photoreactive.

The lakes in our data set remain well mixed on daily cycles primarily due to strong winds (although certainly calm periods occur, enabling stratification and enhancing photochemistry). In this case, daily mixing can reset the photohumification and photodegradation signals (Osburn and Morris 2003), since the ratio of the photic depth (likely a few centimeters given the $K_{d\mathrm{PAR}}$ values in Table 1) to the vertical mixing depth (ranging tens to hundreds of centimeters) controls the amount of photochemistry that occurs. This could explain the poor relationship of S_R to a^*_{350}. However, strong fetch also enables CO_2 emission from surface waters. Therefore, we made estimates of CO_2 flux from the surface of Alkali Lake, based on the photodegradation rate of 207.5 mmol C m^{-3} d^{-1} from previously described experiments in this study. Most UV radiation is attenuated in the top 0.2 m of Alkali Lake (Table 2), so the depth-integrated rate of photodegradation was estimated as 42 mmol C m^{-2} d^{-1}.

Climate implications of prairie lake DOM biogeochemistry—Finally, we place carbon cycling flux estimates in context of recent reports on the importance of saline lakes to global CO_2 flux (Duarte et al. 2008; Finlay et al. 2010). The high pH and alkalinity of saline lakes across the Great Plains mean that most serve as DIC reservoirs, but saline lakes may also release CO_2 through biological respiration and carbonate precipitation (Duarte et al. 2008), while hydrologic inputs of DIC also appear to be important regulators on C fluxes in hardwater lakes (Finlay et al. 2010). Duarte et al. (2008) concluded that carbonate precipitation rather than biological respiration is a driving mechanism for CO_2 supersaturation because of low pCO_2–Chl *a* relationships. Further, they used the Caspian Sea to

Table 7. CO_2 flux estimates for prairie lakes of the U.S. Great Plains, compared with global estimates. Minus sign denotes CO_2 flux into the lake. P : R is the ratio of the rate of PP to the rate of CR. Values < 1 indicate net heterotrophy, hence CO_2 flux to the atmosphere. Fluorescence is in Raman units (R.U.).

CO_2 emission or uptake	Rate (mmol C m^{-2} d^{-1})	Source
Global mean of total release from saline lakes	81–105	Duarte et al. (2008)
Great Plains lakes—CR	median 50 range 26–206	this study; algorithm used was from Cammack et al. (2004)*
Great Plains lakes—PD of autochthonous DOM	median 37 range 4–228	this study†
Great Plains lakes—PP	median −34 range −3 to −483	converted from Salm et al. (2009)
P : R	median 0.86 range 0.06–5.88	this study

* Cammack algorithm: log CR = −1.69 + 0.03R.U. + 0.68 log TP; where R.U. is peak T fluorescence.
† Our photochemical algorithm: PD = (0.36 R.U./2.5 d) × (2.49 g C m^{-3}/0.122 R.U.) × (1000 mmol C/12 g C) × (0.2 m/1); where R.U. is peak M fluorescence.

estimate a global flux of CO_2 from saline lakes at ~120 Tg C yr^{-1} based on CO_2 emission rates of 81 to 105 mmol C m^{-2} d^{-1}. None of these studies consider DOM photodegradation as a contributing factor to CO_2 flux from saline lake surface waters, although our results and those of Waiser and Robarts (2004) clearly demonstrate the importance of photodegradation in saline lake carbon cycles.

To place photodegradation in context of CO_2 dynamics, we calculated rates of photochemical degradation (PD), community respiration (CR), and PP for the lakes in our data set, and compared these rates to CO_2 emission rate estimates (Duarte et al. 2008) (Table 7). PD was estimated using the daily photochemical degradation rate estimate from Alkali Lake, North Dakota, based on the decrease in DOC concentration normalized to the decrease in peak M fluorescence, and integrated over a 0.1-m effective depth. CR was estimated using an algorithm based on peak T and TP data (Cammack et al. 2004). PP was obtained from Salm et al. (2009). Both CR and PP were depth integrated over 1.9 m, the 1% PAR attenuation depth in many of the prairie lakes calculated from K_{d}PAR values (Table 2). Median values are reported along with the range of estimates. The median CR (50 mmol C m^{-2} d^{-1}) was generally higher than the median PP (34 mmol C m^{-2} d^{-1}) in these lakes in May of 2004, although the median ratio of PP : CR (P : R) was 0.86, indicating net heterotrophy in these lakes. The range of all estimates was quite large, indicating the heterogeneity in carbon cycling among the lakes and emphasizing the distribution of these lakes across the color–nutrient paradigm (Fig. 10A,B). PD was high given the relatively shallow depth (0.1 m) used to estimate depth-integrated photochemical production of CO_2. Together, the median CR + PD was 87 mmol m^{-2} d^{-1} and fell within the range of mean CO_2 emission rates estimated for saline lakes globally (Duarte et al. 2008). These preliminary calculations demonstrate that DOM photodegradation in saline lakes can be an important carbon cycling component.

A caveat to these calculations is that the importance of these processes varies with season. For example, photodegradation in prairie saline lakes is maximal during a few summer months and minimal during the winter. Despite these considerations, the high CDOM content in many saline lakes warrants further study of the seasonal uncertainty in the fractional contribution of photochemical and microbial respiration to CO_2 emissions from these systems.

Acknowledgments

We thank two anonymous reviewers for their helpful comments. John Holz, Tadd Barrow, and Danuta Bennett are thanked for field assistance. This work was supported by National Science Foundation Division of Environmental Biology Award 0315665.

References

Anderson, N. J., and C. A. Stedmon. 2007. The effect of evapoconcentration on dissolved organic carbon concentration and quality in lakes of SW Greenland. Freshw. Biol. **52:** 280–289, doi:10.1111/j.1365-2427.2006.01688.x

Arts, M. T., R. D. Robarts, F. Kasai, M. J. Waiser, V. P. Tumber, A. J. Plante, H. Rai, and H. J. de Lange. 2000. The attenuation of ultraviolet radiation in high dissolved organic carbon waters of wetlands and lakes on the northern Great Plains. Limnol. Oceanogr. **45:** 292–299, doi:10.4319/lo.2000.45.2.0292

Biers, E. J., R. G. Zepp, and M. A. Moran. 2007. The role of nitrogen in chromophoric and fluorescent dissolved organic matter formation. Mar. Chem. **103:** 46–60, doi:10.1016/j.marchem.2006.06.003

Birdwell, J. E., and A. S. Engel. 2010. Characterization of dissolved organic matter in cave and spring waters using UV-Vis absorbance and fluorescence spectroscopy. Org. Geochem. **41:** 270–280, doi:10.1016/j.orggeochem.2009.11.002

Blair, N. E., E. L. Leithold, S. T. Ford, K. A. Peeler, J. C. Holmes, and D. W. Perkey. 2003. The persistence of memory: The fate of ancient sedimentary organic carbon in a modern sedimentary system. Geochim. Cosmochim. Acta **67:** 63–73, doi:10.1016/S0016-7037(02)01043-8

Boyd, T. J., and C. L. Osburn. 2004. Changes in CDOM fluorescence from allochthonous and autochthonous sources during tidal mixing and bacterial degradation in two coastal estuaries. Mar. Chem. **89:** 189–210, doi:10.1016/j.marchem.2004.02.012

Cammack, W. K. L., J. Kalff, Y. T. Prairie, and E. M. Smith. 2004. Fluorescent dissolved organic matter in lakes: Relationships with heterotrophic metabolism. Limnol. Oceanogr. **49:** 2034–2045, doi:10.4319/lo.2004.49.6.2034

Cory, R. M., D. M. McKnight, Y. P. Chin, P. Miller, and C. L. Jaros. 2007. Chemical characteristics of fulvic acids from Arctic surface waters: Microbial contributions and photochemical transformations. J. Geophys. Res. **112:** G04S51, doi:10.1029/2006JG000343

Curtis, P. J., and H. E. Adams. 1995. Dissolved organic matter quantity and quality from fresh-water and saltwater lakes in east-central Alberta. Biogeochemistry **30:** 59–76, doi:10.1007/BF02181040

Dillon, P. J., and F. H. Rigler. 1974. Phosphorus-chlorophyll relationship in lakes. Limnol. Oceanogr. **19:** 767–773, doi:10.4319/lo.1974.19.5.0767

Duarte, C. M., Y. T. Prairie, C. Montes, J. J. Cole, R. Striegl, J. Melack, and J. A. Downing. 2008. CO_2 emissions from saline lakes: A global estimate of a surprisingly large flux. J. Geophys. Res. **113:** G04041, doi:10.1029/2007JG000637

Fellman, J. B., E. Hood, and R. G. M. Spencer. 2010. Fluorescence spectroscopy opens new windows into dissolved organic matter dynamics in freshwater ecosystems: A review. Limnol. Oceanogr. **55:** 2452–2462, doi:10.4319/lo.2010.55.6.2452

Findlay, S. E. G., and R. L. Sinsabaugh. 2003. Aquatic ecosystems: Interactivity of dissolved organic matter. Academic.

Finlay, K., P. R. Leavitt, A. Patoine, and B. Wissel. 2010. Magnitudes and controls of organic and inorganic carbon flux through a chain of hardwater lakes on the northern Great Plains. Limnol. Oceanogr. **55:** 1551–1564, doi:10.4319/lo.2010.55.4.1551

Goni, M. A., and S. Montgomery. 2000. Alkaline CuO oxidation with a microwave digestion system: Lignin analyses of geochemical samples. Anal. Chem. **72:** 3116–3121, doi:10.1021/ac991316w

Hedges, J. I., and D. C. Mann. 1979. Characterization of plant tissues by their lignin oxidation products. Geochim. Cosmochim. Acta. **43:** 1803–1807, doi:10.1016/0016-7037(79)90028-0

Heinsalu, A., T. Alliksaar, A. Leeben, and T. Noges. 2007. Sediment diatom assemblages and composition of pore-water dissolved organic matter reflect recent eutrophication history of Lake Peipsi (Estonia/Russia). Hydrobiologia **584:** 133–143, doi:10.1007/s10750-007-8615-2

Helms, J. R., A. Stubbins, J. D. Ritchie, E. C. Minor, D. J. Kieber, and K. Mopper. 2008. Absorption spectral slopes and slope ratios as indicators of molecular weight, source, and photobleaching of chromophoric dissolved organic matter. Limnol. Oceanogr. **53:** 955–969, doi:10.4319/lo.2008.53.3.0955

Hernes, P. J., and R. Benner. 2003. Photochemical and microbial degradation of dissolved lignin phenols: Implications for the fate of terrigenous dissolved organic matter in marine environments. J. Geophys. Res. **108**(C9): 3291, doi:10.1029/2002JC001421

———, A. C. Robinson, and A. K. Aufdenkampe. 2007. Fractionation of lignin during leaching and sorption and implications for organic matter "freshness." Geophys. Res. Lett. **34:** L17401, doi:10.1029/2007GL031017

Kieber, R. J., L. H. Hydro, and P. J. Seaton. 1997. Photooxidation of triglycerides and fatty acids in seawater: Implication toward the formation of marine humic substances. Limnol. Oceanogr. **42:** 1454–1462, doi:10.4319/lo.1997.42.6.1454

Leenheer, J. A., T. I. Noyes, C. E. Rostad, and M. L. Davisson. 2004. Characterization and origin of polar dissolved organic matter from the Great Salt Lake. Biogeochemistry **69:** 125–141, doi:10.1023/B:BIOG.0000031044.16410.27

Louchouarn, P., S. Opsahl, and R. Benner. 2000. Isolation and quantification of dissolved lignin from natural waters using solid-phase extraction and GC/MS. Anal. Chem. **72:** 2780–2787, doi:10.1021/ac9912552

Mariot, M., Y. Dudal, S. Furian, A. Sakamoto, V. Vallés, M. Fort, and L. Barbiero. 2007. Dissolved organic matter fluorescence as a water-flow tracer in the tropical wetland of Pantanal of Nhecolândia, Brazil. Sci. Total Environ. **388:** 184–193, doi:10.1016/j.scitotenv.2007.08.003

Mayer, L. M., L. L. Schick, K. R. Hardy, and M. L. Estapa. 2009. Photodissolution and other photochemical changes upon irradiation of algal detritus. Limnol. Oceanogr. **54:** 1688–1698, doi:10.4319/lo.2009.54.5.1688

McKnight, D. M., E. W. Boyer, P. K. Westerhoff, P. T. Doran, T. Kulbe, and D. T. Andersen. 2001. Spectrofluorometric characterization of dissolved organic matter for indication of precursor organic material and aromaticity. Limnol. Oceanogr. **46:** 38–48, doi:10.4319/lo.2001.46.1.0038

Meybeck, M. 1995. The global distribution of lakes, p. 1–36. *In* A. Lerman, D. M. Imboden, and J. R. Gat [eds.], Physics and chemistry of lakes. Springer-Verlag.

Milbrandt, E. C., P. G. Coble, R. N. Conmy, A. J. Martignette, and J. J. Siwicke. 2010. Evidence for the production of marine fluorescence dissolved organic matter in coastal environments and a possible mechanism for formation and dispersion. Limnol. Oceanogr. **55:** 2037–2051, doi:10.4319/lo.2010.55.5.2037

Nieto-Cid, M., X. A. Álvarez-Salgado, and F. F. Pérez. 2006. Microbial and photochemical reactivity of fluorescent dissolved organic matter in a coastal upwelling system. Limnol. Oceanogr. **51:** 1391–1400, doi:10.4319/lo.2006.51.3.1391

Onstad, G. D., D. E. Canfield, P. D. Quay, and J. I. Hedges. 2000. Sources of particulate organic matter in rivers from the continental USA: Lignin phenol and stable carbon isotope compositions. Geochim. Cosmochim. Acta **64:** 3539–3546, doi:10.1016/S0016-7037(00)00451-8

Ortega-Retuerta, E., E. Pulido-Villena, and I. Reche. 2007. Effects of dissolved organic matter photoproducts and mineral nutrient supply on bacterial growth in Mediterranean inland waters. Microb. Ecol. **54:** 161–169, doi:10.1007/s00248-006-9186-x

Osburn, C. L., and D. P. Morris. 2003. Photochemistry of chromophoric dissolved organic matter in natural waters, p. 185–217. *In* E. W. Hebling and H. E. Zagarese [eds.], UV effects in aquatic organisms and ecosystems. Royal Society of Chemistry.

———, ———, K. A. Thorn, and R. E. Moeller. 2001. Chemical and optical changes in freshwater dissolved organic matter exposed to solar radiation. Biogeochemistry **54:** 251–278, doi:10.1023/A:1010657428418

———, D. W. O'Sullivan, and T. J. Boyd. 2009. Increases in the longwave photobleaching of chromophoric dissolved organic matter in coastal waters. Limnol. Oceanogr. **54:** 145–159, doi:10.4319/lo.2009.54.1.0145

———, and G. St-Jean. 2007. The use of wet chemical oxidation with high-amplification isotope ratio mass spectrometry (WCO-IRMS) to measure stable isotope values of dissolved organic carbon in seawater. Limnol. Oceanogr.: Methods **5:** 296–308, doi:10.4319/lom.2007.5.296

Ouellet, J. F., M. Lucotte, R. Teisserenc, S. Paquet, and R. Canuel. 2009. Lignin biomarkers as tracers of mercury sources in lakes water column. Biogeochemistry **94:** 123–140, doi:10.1007/s10533-009-9314-z

Parlanti, E., K. Worz, L. Geoffroy, and M. Lamotte. 2000. Dissolved organic matter fluorescence spectroscopy as a tool to estimate biological activity in a coastal zone submitted to anthropogenic inputs. Org. Geochem. **31:** 1765–1781, doi:10.1016/S0146-6380(00)00124-8

Romera-Castillo, C., H. Sarmento, X. A. Álvarez-Sarlgado, J. M. Gasol, and C. Marrasé. 2010. Production of chromophoric dissolved organic matter by marine phytoplankton. Limnol. Oceanogr. **55:** 446–454, doi:10.4319/lo.2010.55.1.0446

Salm, C. R., J. E. Saros, S. C. Fritz, C. L. Osburn, and D. M. Reineke. 2009. Phytoplankton productivity across prairie saline lakes of the Great Plains (USA): A step toward deciphering patterns through lake classification models. Can. J. Fish. Aquat. Sci. **66:** 1435–1448, doi:10.1139/F09-083

Sobek, S., L. J. Tranvik, Y. T. Prairie, P. Kortelainen, and J. J. Cole. 2007. Patterns and regulation of dissolved organic carbon: An analysis of 7,500 widely distributed lakes. Limnol. Oceanogr. **52:** 1208–1219, doi:10.4319/lo.2007.52.3.1208

Spencer, R. G. M., and others. 2009. Photochemical degradation of dissolved organic matter and dissolved lignin phenols from the Congo River. J. Geophys. Res. **114:** G03010, doi:10.1029/2009JG000968

Stedmon, C. A., and R. Bro. 2008. Characterizing dissolved organic matter fluorescence with parallel factor analysis: a tutorial. Limnol. Oceanogr.: Methods **6:** 572–579, doi:10.4319/lom.2008.6.572

———, S. Markager, and R. Bro. 2003. Tracing dissolved organic matter in aquatic environments using a new approach to fluorescence spectroscopy. Mar. Chem. **82:** 239–254, doi:10.1016/S0304-4203(03)00072-0

Stets, E. G., and J. B. Cotner. 2008. Littoral zones as sources of biodegradable dissolved organic carbon in lakes. Can. J. Fish. Aquat. Sci. **65:** 2454–2460, doi:10.1139/F08-142

Waiser, M. J., and R. D. Robarts. 2000. Changes in composition and reactivity of allochthonous DOM in a prairie saline lake. Limnol. Oceanogr. **45:** 763–774, doi:10.4319/lo.2000.45.4.0763

———, and ———. 2004. Photodegradation of DOC in a shallow prairie wetland: Evidence from seasonal changes in DOC optical properties and chemical characteristics. Biogeochemistry **69:** 263–284, doi:10.1023/B:BIOG.0000031048.20050.4e

Williamson, C. E., D. P. Morris, M. L. Pace, and O. G. Olson. 1999. Dissolved organic carbon and nutrients as regulators of lake ecosystems: Resurrection of a more integrated paradigm. Limnol. Oceanogr. **44:** 795–803, doi:10.4319/lo.1999.44.3_part_2.0795

Winter, A. R., T. A. E. Fish, R. C. Playle, D. S. Smith, and P. J. Curtis. 2007. Photodegradation of natural organic matter from diverse freshwater sources. Aquat. Toxicol. **84:** 215–222, doi:10.1016/j.aquatox.2007.04.014

Associate editor: Peter Hernes

Received: 03 January 2011
Accepted: 03 August 2011
Amended: 19 August 2011